

Graphics are disabled. Document is incomplete.
Enable graphics by using `\graphicstrue` in `main.tex`.

Master's Thesis



F3 Faculty of Electrical Engineering
Department of Computer Graphics and Interaction

SIMR

**Simulating the phenomena of altered states
of consciousness using virtual reality**

Jakub Hlusička

2021–2022

Supervisor: Ing. Josef Kortan

Diplomová práce



Fakulta elektrotechnická
Katedra počítačové grafiky a interakce

SIMR

Simulace fenoménů pozměněných stavů v domí pomocí virtuální reality

Jakub Hlusička

2021–2022

Školitel: Ing. Josef Kortan

Abstract

TODO English AND Czech required!!!

Acknowledgements

I would like to thank the following people, in no particular order:

My supervisor, Ing. Josef Kortan, for his willingness to supervise my work and undergo the formalities surrounding it, and his continued supply of encouragement.

My previous supervisor, Ing. David Sedláček, Ph.D., for his willingness to let me explore a variety of topics under his supervision, while I was still uncertain about the topic of my master's thesis.

The Department of Computer Graphics and Interaction at FEL CTE, and Ing. David Sedláček, Ph.D. in particular, for making the VR laboratory accessible for the development of the application and for the evaluation of the application, during which I conducted a study in the VR laboratory over the course of 2 weeks.

Mgr. et Mgr. Iveta Fajnerová, Ph.D., for her invaluable input during the initial stage of the project and her willingness to mentor me through the process of designing the study for the evaluation of the developed application.

The developers of the *iTrip* application, and MUDr. Filip Tylš, Ph.D. in particular, for providing the czech translation of the psychometric questionnaire.

Dr. Timo Torsten Schmidt, for his mentorship regarding the scoring of the psychometric questionnaires.

Ossi Luoto, Fabrice Piquet, Jason Hoku, and Ing. Ondřej Slabý, for their invaluable advice regarding development in Unreal Engine 4.

The generous participants of the study, who were offered no financial or material compensation for their time.

Alexandra Elbakyan for founding and her continued maintenance of the Sci-Hub website, without which this endeavour would have most definitely been impossible. After all, *we are standing on the shoulders of giants*.

Finally, I would like to thank my parents for their continued support throughout my pursuit of advanced studies.

—Jakub Hlusička

“Not everything that is faced can be changed, but nothing can be changed until it is faced.”

—James Baldwin, *As Much Truth as One Can Bear* (1962)

Declaration

I declare that the presented work was developed independently and that I have listed all sources of information used within it in accordance with the methodical instructions for observing the ethical principles in the preparation of university theses.

Prohlašuji, že jsem předloženou práci vypracoval samostatně a že jsem uvedl veškeré použité informační zdroje v souladu s Metodickým pokynem o dodržování etických principů při přípravě vysokoškolských závěrečných prací.

Prague, 20. 5. 2022

Contents

1	Introduction	1
1.1	Problem Statement	1
1.2	Motivation	1
1.2.1	Art and Media	1
1.2.2	Education	1
1.2.3	Research and Psychotherapy	1
1.2.4	Understanding of the Human Mind	2
1.3	Related Work	3
1.3.1	Recreations of Visual Phenomena	3
1.3.1.1	Quake Delirium	3
1.3.1.2	Crystal Vibes feat. Ott.	4
1.3.1.3	Isness	5
1.3.1.4	Hallucination Machine	7
1.3.1.5	Lucid Loop	8
1.3.1.6	Other AI-based Approaches	8
1.3.2	Tactile Stimulation Interfaces	9
1.3.2.1	Synesthesia Suit for Rez Infinite	10
1.3.2.2	Synesthesia X1 - 2.44	10
1.3.2.3	Subpac	10
1.4	Contributions	10
2	Background	11
2.1	Altered States of Consciousness	11
2.1.1	Phenomenology of Psychedelic States	11
2.1.2	Aspects	12
2.1.3	Replications	12
2.2	Psychometric Evaluation Methods	13

3	Implementation	14
3.1	Design of the Application	14
3.1.1	Safety	14
3.1.2	Interaction	15
3.1.3	Virtual Scene Creation	15
3.2	Implementation of Replications	16
3.2.1	Spatial Effects	16
3.2.1.1	Depth Perception Distortion	16
3.2.1.1.1	First Attempt	17
3.2.1.1.2	Final Solution	17
3.2.1.2	Visual Drifting	20
3.2.2	Non-Spatial Effects	22
3.2.2.1	Visual Acuity Enhancement	23
3.2.2.1.1	Enhancement of Saturation and Contrast	23
3.2.2.1.2	Enhancement of Texture Detail via Sharpening	23
3.2.2.2	Tracers	24
3.3	Complex Replication	25
3.3.1	Execution Order	25
3.3.2	Experiment Automation and Controls	26
4	Evaluation	30
4.1	Methods	30
4.2	Results	32
5	Conclusion	33
5.1	Discussion	33
5.2	Limitations	33
5.3	Future Work	34
	Bibliography	42
A	Questionnaire	43
B	Informed Consent Form	46
C	Remarks on the Method of Statistical Analysis	48

1 | Introduction

1.1 Problem Statement

This thesis is focused on the development of a virtual reality (VR) application that simulates select aspects of altered states of consciousness (ASCs; further defined in 2.1) typically induced by classical, serotonergic (acting on the 5-HT receptors) psychedelics, such as LSD, psilocybin/psilocin, or DMT. We focus primarily on the recreation of the ASCs' effects on sensory perception using an analytical approach.

1.2 Motivation

Due to their high degree of immersion, VR systems, with head-mounted displays (HMDs) in particular, offer a unique opportunity for recreating certain aspects of ASCs.

1.2.1 Art and Media

ASCs of various forms have had a significant influence on art for millennia. Earliest signs of inductions of ASCs via neurotropic substances have been found possibly as early as 60,000 BC (Guerra-Doce 2015). ASCs continue to be depicted in or influence contemporary popular media.

An analysis and a recreation of certain aspects of ASCs may serve as a reference point for recreating those aspects of ASCs in popular media.

1.2.2 Education

While experiencing a simulation of an ASC is unlikely to be fully representative of the ASC the simulation is modelled after, we propose that the simulation may be significantly less inductive of difficult experiences colloquially known as "bad trips".

This may be a viable alternative form of experiencing certain aspects of ASCs, while the possession or consumption of mind-altering substances is illegal in most countries. The resulting VR application may serve as an educational tool about ASCs which would not require as controlled of an environment as is required in psychedelic-assisted psychotherapy.

1.2.3 Research and Psychotherapy

Aday, Davoli, and Bloesch (2020) make an interesting observation, that psychedelics and VR are utilized in tandem to enhance the experience of recreational users. Moreover, the

authors claim that VR could also be used to optimize and tailor the therapeutic setting during psychedelic sessions.

Most importantly, however, the authors state, that:

[...] VR may be a useful tool for preparing hallucinogen-naïve participants in clinical trials for the sensory distortions experienced in psychedelic states.

Nonetheless, as mentioned previously, care should be taken to ensure that users experiencing the simulation are informed about the simulation not being fully representative of the *ASC* it is modelled after. While a *VR* simulation may be suitable for simulating sensory effects of *ASCs*, other effects, such as the effects on cognition, may be much more difficult, if not impossible, to directly replicate via *VR* technologies alone. If uninformed, users may gain a false impression about the *ASC*.

Greco et al. (2021) propose that simulated hallucinations may be used to investigate neural mechanisms of conscious perception without difficulties posed by pharmacologically-induced *ASCs* — namely the ethical and legal issues, as well as the difficulty to isolate the neural effects of psychedelic states from other physiological effects elicited by the drug ingestion. The study used *DeepDream* (Mordvintsev, Olah, and Tyka 2015) to generate hallucinations by modifying a video clip.

[Their] findings suggest that *DeepDream* and psychedelic drugs induced similar altered brain patterns and demonstrate the potential of adopting this method to study altered perceptual phenomenology in neuroimaging research.

Very recent research (Rastelli et al. 2021) indicates that simulated altered perceptual phenomenology enhances cognitive flexibility and inhibits automated decision making. The study describes cognitive flexibility as “the ability to shift attention between competing concepts and alternative behavioral policies to meet rapidly changing environmental demands”.

1.2.4 Understanding of the Human Mind

Finally, without any immediate application, the study of the effects of *ASCs* may help contribute to our understanding of the human mind. Particularly, for instance, analyzing the invariant effects of classical psychedelics on sensory perception may improve our understanding of the visual cortex and the way it functions. Further research involving perceptual phenomena and pharmacodynamics of psychedelics and their mechanisms of action may contribute to our understanding of the significance of certain receptors in processing visual or other sensory information.

The problem of understanding consciousness has long been of interest to philosophers (Block 1993), neuroscientists (Crick and Koch 1990), as well as cognitive psychologists (Dehaene 2014). Recently, with the resurgence of deep neural networks, attempts to contribute to our understanding of consciousness have also appeared in the field of artificial intelligence (*AI*) (Bengio 2017; Reggia, Katz, and Davis 2020). One such study (Bensemman and Witbrock 2021) examined the effects of implementing phenomenology (in a broader sense of the word, not psychedelic) into a deep neural network.

1.3 Related Work

1.3.1 Recreations of Visual Phenomena

In this section, we explore the way *ASCs* have been depicted in contemporary art and media and recent attempts at recreating aspects of *ASCs* in the scientific domain.

1.3.1.1 Quake Delirium

In the original paper about Quake Delirium (Weinel 2011), the author divides video games portraying *ASCs* into two categories:

1. Games which feature literally portrayed dreams, intoxication or hallucinogenic experiences.
2. Games which feature graphical or thematic content which audiences may consider to reflect states of dream, intoxication or hallucination, but without any direct or literal reference to these states.

This categorization is not only useful for examining video games, but also the rest of art and media.

The first category describes media that attempts to recreate *ASCs* with an explicit reference to a specific induction method, cause or origin. For example, the games in this category, such as Grand Theft Auto: Vice City¹ or Duke Nukem 3D², may temporarily portray a character under the influence of a psychoactive drug. However, psychoactive substances are not the only form of *ASC* induction portrayed in video games. One such exception is LSD: Dream Emulator³, a game with narrative based on a dream diary and an overall dream-like surrealist aesthetic.

The second category contains media that does not communicate explicitly any *ASC* method of induction, cause or origin. Despite this, the media that falls into this category may be viewed equally as *psychedelic* or more than that of the first category. This could be considered to be the case of Yoshi's Island⁴. While the creators may not have intended the video game to reflect *ASCs*, because of its brightly colored surrealistic visual themes, it may resemble *ASCs* of games from the first category.

The *Quake Delirium* project itself is a modification of the game *Quake* that makes use of an external digital signal processing (*DSP*) audio patch for modifying the resulting audiovisual output the game produces. The visual effects consist of changes in:

1. field of view (*FOV*);
2. camera swaying;
3. fog density and color;
4. game speed;
5. stereo vision (for 3D red cyan glasses);
6. gamma;
7. hue.

¹Grand Theft Auto: Vice City, Rockstar Games, 2003. PC (Windows) CD-ROM.

²Duke Nukem 3D, 3D Realms, 1996. PC (Windows) CD-ROM.

³LSD: Dream Emulator, Asmik Ace Entertainment, 1998. Playstation.

⁴Super Mario World 2: Yoshi's Island, Nintendo, 1995. Super NES.

These visual effects are made available to the **DSP** patch, the control of which can be automated using multi-track audio sequencing software. This enables the effects to onset slowly and gradually become more severe over time.

The project demonstrates a method of combining multiple partial effects that results in a complex audio-visual effect that is more sophisticated than many of the existing games exhibiting phenomena of **ASCs** surveyed.

Interestingly, the authors went on to experiment with a dynamic way of controlling the intensity and parameters of the simulated effects in a follow-up study (Weinel et al. 2015). Rather than controlling the parameters using a *pre-determined automation path* via multi-track audio sequencing software, this modification introduced biosensor as a way of influencing the simulation parameters – specifically, they used the commercial *NeuroSky Mind-Wave* electroencephalograph (**EEG**) device. The study ultimately concludes, that “while the use of EEG to control psychedelic visual effects is conceptually appealing, the current system would also need to be improved to provide a more tangible connection between the headset and the ASC effects in the game.”

There is no straightforward way to map **EEG** signals onto visual effects. The **EEG** signals need to be interpreted, so that relevant information is extracted. Mapping the extracted information onto specific simulation parameters is then at the artist’s discretion. A more sophisticated approach might examine correlations between observed **ASC** phenomena and **EEG** signals, then use those correlations to model the mapping from **EEG** signals onto the visual effects.

1.3.1.2 Crystal Vibes feat. Ott.

Outram et al. (2017) describe *Crystal Vibes feat. Ott.* as a project originally developed to demonstrate the full-body vibrotactile *Synesthesia Suit*, further discussed in 1.3.2.1. The experience places the user into an abstract geometric environment procedurally generated from a soundtrack:

Crystal Vibes does not use any 3D modelling, 2D design, or hand animation. Instead, the environment is generated using sine and Bézier functions, Bravais lattice structures and Fourier transforms of the audio. Crystal Vibes exploits the innate beauty of 3-dimensional crystal structures, and leverages the artistry of rhythm and form in the music for visual beauty.

The article describes in detail the methods employed to simulate audiovisual synesthesia using sound visualization, with an attempt to be “as physically and biologically defensible as possible”. The methods include compensation for the non-linear perception of both auditory and visual information:

This includes the fact that humans perceive equal pitch differences corresponding roughly to equal differences in the log of audible frequency, that our perception of volume varies over the audible range, and how humans interpret colour from a visible spectrum.

Another technique used to aid in distinguishing different voices of the soundtrack, such as drums and synths, is spatial separation. Each voice would impact a separate region of the visualization. This way, the user can form an association between spatial regions and their corresponding voices.

Finally, the last employed technique of improving the perception of sound via sight is to provide temporal information; instead of only visualizing the current instant of the soundtrack, a roughly 1 second long moving slice of the soundtrack is visualised.

The authors report that users found the visualization compelling, even those who experience synesthesia in their daily lives. Synesthesia is of our interest because it is a prominent phenomenon of some *ASCs*.

1.3.1.3 *Isness*

The paper (Glowacki et al. 2020) accompanying the project *Isness* proposes that so-called ‘mystical-type’ experiences (*MTEs*), that are often experienced under the influence of psychedelic drugs, may also be facilitated by virtual reality. The paper justifies this proposal by conducting a study with 57 participants analyzing participants’ responses to the 30-item revised mystical experience questionnaire (*MEQ30*), commonly used to evaluate the effects of psychedelic drugs. The results of the study indicated that *Isness* participants reported *MTEs* comparable to those reported in double-blind clinical studies after high doses of psilocybin and lysergic acid diethylamide (*LSD*).

The *VR* application was designed to be used by 4 participants at a time with the *HTC Vive Pro HMDs*. To provide multiplayer functionality, the client/server architecture was chosen, with each *HMD* being connected to a separate *GPU*-accelerated server.

The abstract virtual environments have been designed by defining a set of ‘aesthetic hyperparameters’, each affecting a different aspect of the simulated *MTE*. The overall *Isness journey* was comprised of a set of states, each of which had some specific time duration. This approach allowed for reproducibility necessary for the study.

Participants were equipped with specially-made ‘Mudra gloves’, which would create a light source within the virtual scene when they made a ‘mudra pose’ by bringing the tip of a thumb to their forefinger or middle finger.

The entire *Isness journey* was divided into 3 phases:

1. Phase 1: Preparation. 15-20 minutes, included information about practical issues (phones off, toilet locations, placing possessions in a safe place), screening, description of the experience, information that the participants could withdraw at any point, and acquisition of verbal and written consent for participation in the study. This phase also included some group exercises to build rapport between participants.
2. Phase 2: Multi-person *VR* session. 35 minutes with a pre-recorded narrative soundtrack. The *VR* experience was preceded by a blindfolded, narrated group meditation. Each participant was then fitted with a VR headset and the administrator initiated the *VR* session, moving through 15 prespecified states, each composed from a set of aesthetic hyperparameters.
3. Phase 3: Integration. The *HMDs* were taken off. Breath exercises and group exercises followed. Participants were then invited to share in a 10-15 minute facilitated discussion, after which they were provided a blank piece of paper for reflective writing, along with a blank *MEQ30*.

⁵© Outram et al. (2017), permission for use granted by the authors.

⁶© Outram et al. (2017), permission for use granted by the authors.

(a)
A
screen-
shot
from
the
first
main
part
of
*Crys-
tal
Vibes*,
with
an
adap-
tive
mesh
that
en-
velops
the
user
and
re-
sponds
vi-
su-
ally
to
the
mu-
sic.⁵

(b)
A
screen-
shot
from
the
sec-
ond
main
part
of
*Crys-
tal
Vibes*,
in
which
sound
vi-
su-
al-
i-
sa-
tion
in
the
form
of
colour
flows
through
an
end-
less
lat-
tice
of

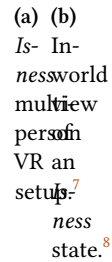


Figure 1.2: Design of the *Isness* VR application.

It is fair to say that the *Isness* project focuses mainly on the replication of *MTEs*, whose characteristics include a sense of connectedness, transcendence, and ineffability; specifically the effects of *ASCs* on emotion and cognition, rather than the effects on sensory perception, as is also evident by the *MEQ30* questionnaire used in the study. This can be seen in the emphasis on the narrated structure of the *Isness journey*, the inclusion of a meditation session, as well as in the multiplayer design of the overall experience, that encourages interaction between participants.

That is to say, the *Isness journey* has been effective in creating a memorable, subjectively meaningful experience comparable to *ASCs* induced by psychedelic drugs.

1.3.1.4 Hallucination Machine

Hallucination Machine (Suzuki et al. 2018) makes use of the *DeepDream* (Mordvintsev, Olah, and Tyka 2015) technology to alter spherical panoramic video. The altered video is then viewed through a *HMD*. The usage of *DeepDream* successfully simulates the sense of an increased ability to recognize patterns during certain *ASCs*.

While it is a compelling concept, there are many drawbacks to this approach.

1. The alteration caused by *DeepDream* is heavily dependent on the source data the deep convolutional neural networks (*DCNN*) is trained with. If, for example, the *DCNN* is trained with images of puppies, the alteration by this *DCNN* will result in *hallucinated* puppies.
2. The panoramic spherical videos are not stereoscopic, hence the sense of depth is lost.
3. Finally, the fact that the *DeepDream* technology is computationally demanding may have resulted in the choice to use pre-recorded videos rather than real-time footage. This, however, limits the applications of the solution.

However, what the *DeepDream* technology does well is the simulation of the sense of an increased ability to recognize patterns, otherwise known as pareidolia, characteristic of certain *ASCs*. For this reason, it has found popular use in research as a way to simulate hallucinations (Greco et al. 2021; Rastelli et al. 2021).

⁷A cropped version with label removed of “Isness multi-person VR setup” released by Glowacki et al. (2020) under the CC BY-SA 4.0 license. © Glowacki et al. (2020).

⁸A cropped version with label removed of “In-world view of an Isness state” released by Glowacki et al. (2020) under the CC BY-SA 4.0 license. © Glowacki et al. (2020).

⁹Released by Martin Thoma under the CC0 1.0 (public domain) license.

¹⁰Released by Martin Thoma under the CC0 1.0 (public domain) license.

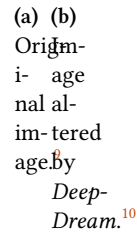


Figure 1.3: Example result of applying the *DeepDream* technology to an image.

1.3.1.5 Lucid Loop

Lucid Loop (Kitson, DiPaola, and Riecke 2019) is a proposed VR application that makes use of an EEG device (along with other biosensors) for biofeedback. The application is a proposed training aid for maintaining awareness during lucid dreaming, a state reached when a person becomes aware they are dreaming.

The application makes use of a HMD to display *DeepDream*-altered (Mordvintsev, Olah, and Tyka 2015) content with the intensity of alteration corresponding to the current brain wave distribution of the wearer — as higher frequency brain waves dominate, the displayed content becomes less affected by *DeepDream*, resulting in more clarity; as lower frequency brain waves dominate, the displayed content becomes more affected and is interpreted as more dreamy and abstract.

The concept is promising, but the choice of *DeepDream* might prove to be challenging to implement effectively, as the intensity of the *DeepDream* alteration of displayed content is dynamic. The *DeepDream* algorithm would either have to be applied in real-time, which is problematic due to the algorithm’s high computational demands, or an optimization scheme would have to be used. One such optimization scheme, assuming spherical panoramic video as displayed content, might pre-render the video as altered by *DeepDream* for several levels of intensity, and then during usage, would interpolate between the pre-rendered videos.

Finally, while the tool is supposed to aid in helping maintain awareness during lucid dreaming, I find it to be a missed opportunity, that the paper does not address the event that high frequency brain waves, while perhaps corresponding to greater awareness, might also cause the dreamer to wake up. A possible improvement of this tool might take this into consideration and also provide biofeedback for this event, such as fading the displayed content to white as the user becomes “too aware”.

1.3.1.6 Other AI-based Approaches

Schartner and Timmermann (2020) develop two models for generating image distortions reminiscent of verbal reports from clinical trials of *N,N*-dimethyltryptamine (DMT).

In the first approach, the authors employed the *StyleGAN* algorithm (Karras, Laine, and Aila 2019) and modified it such that no noise input was added during the generation process, according to a hypothesized brain mechanism. This resulted in smoother, painterly look of the images.

In the second approach, the authors used the *Fast Neural-Style Pytorch Implementation for Artistic Style Transfer* (Johnson, Alahi, and Fei-Fei 2016). This method allows for the

(a)	(b)
Ef-	Ef-
fect	fect
of	of
Style-	a
GAN	style
with	trans-
vary-	fer
ing	net-
lev-	work
els	with
of	vary-
noise. ¹¹	ing
	lev-
	els
	of
	bias. ¹²

Figure 1.4: Results from the modification of *StyleGAN* and the usage of a style transfer network.

depiction of nearly any report of a visual hallucination, assuming one can find a matching content and style image.

1.3.2 Tactile Stimulation Interfaces

VR interfaces provide a way to replace sensory information with information provided by the **VR** application. Different kinds of interfaces have been developed since the conceptualization of **VR**, but among the most practical and commercially available is the **HMD**, which includes stereoscopic screens for visual information, and usually provides a way to substitute auditory information as well, either by providing built-in headphones or an audio connection to connect external headphones to. The main purpose of these interfaces is to provide (or improve the amount of) immersion within the virtual scene.

Among other **VR** interfaces, *tactile stimulation interfaces* deserve a special mention, because of their relevance to the simulation of **ASCs**, in particular, the simulation of haptic and auditory synesthesia, and because of their past usage in related projects. In this section, we mention several of these interfaces.

¹¹A cropped version of “NVIDIA’s generative model with noise perturbation and analogous hypothesized brain mechanism” released by Schartner and Timmermann (2020) under the **CC BY-SA 4.0** license. © Schartner and Timmermann (2020).

¹²“Example output of a style-transfer network” released by Schartner and Timmermann (2020) under the **CC BY-SA 4.0** license. © Schartner and Timmermann (2020).

1.3.2.1 Synesthesia Suit for Rez Infinite

The *Synesthesia Suit* (Konishi, Hanamitsu, Outram, Minamizawa, et al. 2016; Konishi, Hanamitsu, Outram, Kamiyama, et al. 2016; Synesthesia Lab 2016) is a full-body suit that provides haptic sensation via 24 actuators, all of which can be independently controlled. The suit has been developed for the VR game *Rez Infinite* (Enhance Experience Inc. 2016). The aforementioned VR game *Crystal Vibes feat. Ott.* (see 1.3.1.2; Outram et al. (2017)) has been developed to demonstrate the capabilities of this suit.

Figure 1.5: The *Synesthesia Suit*.¹³

In the game *Rez Infinite*, the suit would provide feedback for interactions like shooting, hitting, and warping. The suit would respond to collisions in the virtual world, as well as to the in-game action and sounds.

The design of the *Synesthesia Suit* was later improved by *Synesthesia Wear* (Furukawa et al. 2019), which adds wireless connections and improves user intuitiveness and customizability in the placement of the actuators.

1.3.2.2 Synesthesia X1 - 2.44

Synesthesia X1 - 2.44 (Synesthesia Lab 2021) is a seat with 2 speakers and 44 vibrotactile actuators. While it has been presented without a HMD, the possibility of using a HMD while seated is available, but the design of this tactile interface as a seat makes it impossible for the user to move around. Still, it might be suitable used for the development of a more passive VR experience.

1.3.2.3 Subpac

Commercial wearable subwoofers, such as the *Subpac* (SUBPAC 2013), are able to have a significant impact on immersion (Drempetic and Potter 2017) even for non-VR content.

The *Subpac* has been used in *Longing for Wilderness* (Zimmermann, Helzle, and Arellano 2016), a VR experience that “takes you from the noisy city through the slowly transforming forest towards a calm and airy landscape”. The sound design of the application has been specially made with the device in mind.

1.4 Contributions

We develop a VR application for HMDs that simulates select aspects of ASCs. We perform a study in which we measure the influence of the created VR application on the human mind. This measurement is done via the 11-Factor Altered States of Consciousness Questionnaire (11-ASC; Studerus, Gamma, and Vollenweider (2010)) and the 5-Dimensional Altered States of Consciousness Questionnaire (5D-ASC; Dittrich, Lamparter, and Maurer (2010)) used in clinical studies of ASCs induced by psychedelic drugs, and other kinds of ASCs.

¹³© Konishi, Hanamitsu, Outram, Kamiyama, et al. (2016), permission for use granted by the authors.

2 | Background

2.1 Altered States of Consciousness

Ludwig (1966) define ASCs as „any mental state(s), induced by various physiological, psychological, or pharmacological maneuvers or agents, which can be recognized subjectively by the individual himself (or by an objective observer of the individual) as representing a sufficient deviation in subjective experience or psychological functioning from certain general norms for that individual during alert, waking consciousness.“

This term is meant to encompass phenomena such as sleep, dream states, day dreaming, hypnosis, sensory deprivation, hysterical states of dissociation and depersonalization, pharmacologically induced mental aberrations and so on, and provide a framework for further analysis of these phenomena.

With regards to psychedelics specifically; ASCs induced by psychedelics are mainly characterized by profound alterations in sensory perception, mood, thought including the perception of reality, and the sense of self (Preller and Vollenweider 2016).

2.1.1 Phenomenology of Psychedelic States

The main component of the psychedelic experience is the concept of the *phenomenological ego* and the way it is influenced throughout the experience.

According to Metzinger (2009), the ego is the content of a self-model; this conscious self-model constructed by the brain allows us to interact with our internal world as well as with the external environment in a holistic manner. In a broad sense, the self encompasses features such as a first-person perspective, feelings of agency, ownership (“mineness”) and immediacy (“nowness”), spatial perspective, autobiographical memory, emotions, perceptions, thoughts and acts of will, as well as the feeling of being embedded in our bodily sensations (Metzinger 2009; Northoff 2011).

Another function of the ego serves is to help control and plan our behavior and to understand the behavior of others. By representing the process of representation itself, we can catch ourselves in the act of knowing. Ultimately, the subjective experience of the ego arises from dynamic self-related information processing, which is the result of a self-organizing brain system interacting with its environment, because no such things as selves exist in the world (Metzinger 2009). (Preller and Vollenweider 2016)

According to Masters and Houston (2000), modified by Preller and Vollenweider (2016), the suppression of the *phenomenological ego* during the results in distinctive stages of the

psychedelic experience, with alterations at:

1. The perceptual level: Most frequent and robust features of the psychedelic experience. Perceptual effects are dominated by visual phenomena. Transformation of the environment and alterations of the body image are frequently reported.
2. The recollective-psychodynamic level: Visual images become more personalized, and boundaries between consciousness and unconsciousness dissolve, causing recall and re-enacting of past experiences and memories and releasing emotions into the process.
3. The symbolic existential level: More personal involvement and emotional engagement is develop during this stage. Subjects become more personally involved and emotionally engaged as a participant in the ongoing psychedelic scenario.
4. **The deep integral level of self-transcendence:** Along with the increasing dissolution of the ego, the psychedelic experience can peak in a state where subjects can become immersed for seconds or minutes in a profound awareness of oneness in which all boundaries disappear and objects are unified into a totality.

(Preller and Vollenweider 2016)

The intensity and duration of the psychedelic experience depends most critically on the dosage, the specific drug, and the route of administration. However, other factors, such as personality structure, the nature and dynamics of unconscious material activated, the setting (physical, cultural, and social environment) in which the experience takes place, and the expectancy of the subject are also important (Preller and Vollenweider 2016). See figure 2.1.

Figure 2.1: Temporal dynamics and stages of a psilocybin-induced psychedelic experience. Adaptation by Preller and Vollenweider (2016) of the original by Leuner (1962).

2.1.2 Aspects

For the purpose of this thesis, we define an *aspect* of an **ASC** as a single, distinctive phenomenon of an **ASC**. An *aspect* does not describe the entirety of the **ASCs**, only a particular part of it. In order to model **ASCs**, we analyze them and break them down into their respective *aspects*.

An example that is common for **ASCs** induced by psychedelics is the distortion in the perception of time.

2.1.3 Replications

Replications are recreations or simulations of one or more aspects of **ASCs** using various forms of media (audio, video, tactile, etc.) with the intention of communicating the experience of **ASCs**. Many examples are described in section 1. Various artistic *replications* may be viewed at PsychonautWiki (2021).

For the rest of this thesis, a *replication* will refer to a recreation or simulation of a *single* aspect of **ASCs**. Furthermore, a *complex replication* will refer to a combination of *replications*.

A *replication* of time perception distortion may be simulated via the augmentation of the playback speed of a videoclip using non-linear resampling, or via the augmentation of the

simulation speed (timestep) of a **VR** application. This augmentation may be performed by replacing the original sampling function $s: \mathbb{R} \rightarrow \mathbb{R}$ by $s'(t) = s(t) + f(t)$ where $f: \mathbb{R} \rightarrow \mathbb{R}$ is a function for sampling procedurally generated noise, such as Perlin noise (Perlin 1985) or Simplex noise (Olano et al. 2002).

2.2 Psychometric Evaluation Methods

Psychometric evaluation of **ASCs** is generally performed via questionnaires, of which there are many available. Schmidt and Majić (2018) and Figueiredo et al. (2016) performed an analysis of 9 such questionnaires and recommends the 5-Dimensional Altered States of Consciousness Questionnaire (**5D-ASC**), 11-Factor Altered States of Consciousness Questionnaire (**11-ASC**) and the Phenomenology of Consciousness Inventory (**PCI**) questionnaires for general assessment of **ASCs**.

The **11-ASC** was chosen over the **PCI** due to the popularity of the **11-ASC** in the evaluation of psychedelic-induced **ASCs**, and because of the complete lack of **VR**-related studies using the **11-ASC**.

Additionally, the **11-ASC** uses a subset of questions of the **5D-ASC**, both of these questionnaires can be therefore understood as different scorings of the same set of questions. For this reason, the **5D-ASC** scorings are also included in our study.

A czech translation of the questionnaire was used. The translation was kindly provided by the developers of the *iTrip* smartphone application (Filip Tylš 2020), developed by **PSYRES**¹ (a czech foundation for psychedelic research) in partnership with **CZEPS**² (Czech Psychedelic Society), and was corrected for spelling mistakes and formatting consistency. Unfortunately, we are not aware of any czech translation that has been statistically validated, and for the purpose of this thesis, we assume the used translation (see appendix A) is statistically valid.

¹<https://web.archive.org/web/20220504111203/https://psyres.eu/>

²<https://web.archive.org/web/20220504110718/https://czeps.org/>

3 | Implementation

The objective of this part of the project was to implement an immersive replication of *ASCs* induced by classical psychedelics. In order to achieve a high degree of immersion, our solution was designed to be intended for immersive *VR* systems with *HMDs*. Our solution will be referred to with “*the application*” or “*our application*” for the rest of this document.

To represent the *ASCs* of classical psychedelics objectively, we had to resort to modelling only the “perceptual level” stage of the psychedelic experience (as seen in figure 2.1), as further stages require subjective personalization of content, and aspects less suitable for replication via immersive *VR*, such as cognitive effects and the suppression of the *phenomenological ego*.

3.1 Design of the Application

The application was designed primarily for the evaluation of the implemented replication. The development of the application consisted of 3 distinct parts:

1. **The environment:** A virtual scene that should look as realistic as possible.
2. **The replication:** Implementation of the effects themselves.
3. **Adaptation for testing:** Getting the application ready for a study, that might measure the impact of the replication on the human mind.

3.1.1 Safety

In order to ensure our application’s users safety, we have consulted the *Recommendations for good scientific practice and the consumers of VR-technology* (Madary and Metzinger 2016). The application was developed according to these recommendations.

Mainly, we don’t expect the developed application to have lasting traumatic effects on the users; instead, we believe that this medium may be a suitable way to explore aspects of psychedelic-induced *ASCs* while minimizing those risks.

Further, we’ve taken safety and intuitiveness into account while designing the controls and choosing a suitable testing area for experimentation with *VR* (the “*VR play space*”).

Finally, the application must be automated, so that the administrator may assist the user and ensure their safety during the usage of the application.

3.1.2 Interaction

Interaction with the scene via hand-held controllers was removed entirely, as we felt that the currently available consumer VR technology does not implement a realistic, consistent, universal and intuitive solution for interaction with the virtual scene. For example, in VR applications, interactions are usually implemented so that if a user takes a hand-held controller to a dynamic physics-enabled object, they may be able to pick it up by pressing or holding a trigger on the hand-held object, which makes the object stick or snap to the virtual representation of the controller in the scene. While this solution may be suitable for VR games, it is still understood as a simplification.

As an alternative, one may consider using force feedback haptic gloves, and given a sufficient physically based simulation, it may be possible to implement realistic interactions with virtual objects. However, even such gloves apply force feedback only to the fingers and not the entire body, making it impossible to, for example, lean against virtual objects.

In any case, no such force feedback haptic gloves were available to us for this project, and so interaction was entirely foregone, in the interest of keeping the simulation focused mainly on the replication, rather than an unrealistic implementation of interactions.

3.1.3 Virtual Scene Creation

Given the goal of creating as realistic of a scene as possible, as well as no financial budget for this project, we ended up choosing Unreal Engine 4 (UE4)¹ as the game development engine to develop our VR application with. UE4 is free to use for projects with a lifetime gross revenue below \$1 million USD, and we have no plans to monetize it. Additionally, the choice of UE4 makes it possible to use the Quixel Megascans² 3D asset library for free within UE4, due to special licensing as a result of the acquisition of Quixel by Epic Games³, the developer of UE4.

The virtual scene was created with the intended VR *play space* in mind, which was measured to be about $3.5 \times 3.5 \text{ m}^2$ large. The virtual scene contains visual cues of the *play area* borders in the form of 3D assets; specifically, the *play area* is surrounded by a railing and tall rock, communicating to the user, that these objects should not be passed through.

The choice was made to create an outdoor scene, as the surrounding nature might provide a more pleasant environment than an indoor scene. However, our implementation is in no way limited to outdoor scenes only.

At first, we attempted to create a forest scene, but quickly ran into performance issues while trying to render a densely populated forest on a HMD, which requires at least 2 views rendered at typically higher resolutions than a regular desktop screen, ideally with at least 90 FPS (the native refresh rate of the HMD). Delivering a consistent framerate is a requirement, as low framerates and stuttering may cause motion sickness.

It was then decided to abandon the idea of a forest scene and, instead, use a high dynamic range imaging (HDRI) panoramic photograph as a background (hereinafter “panoramic background”) for the scene. It is important to note, that a panoramic background has no depth information. This drawback can be mitigated by making only the very distant parts of the panoramic background visible to the user, so that the illusion of the panoramic

¹<https://web.archive.org/web/20220514231756/https://www.unrealengine.com/en-US>

²<https://web.archive.org/web/20220514233901/https://quixel.com/megascans>

³<https://web.archive.org/web/20220514235540/https://www.epicgames.com/site/en-US/home>

background being realistic is not broken. The illusion relies on the fact that binocular disparity is low for distant objects.

Close parts of the panoramic background can be hidden with 3D assets suitable for the environment. To minimize the area that needed to be hidden, we have chosen a mountainside panoramic background (see figure 3.1).

Figure 3.1: The chosen panoramic background “Canon”⁴ available on Poly Haven⁵.

The final scene contains a flat patch of grass and other low foliage the size of the *play area*, containing a wooden bench with some gardening tools. The grass patch is surrounded with rock formations and a rocky stairway leading towards it. Beyond the railing, there is a nice view of the sea cove.

Figure 3.2: A preview of the resulting scene.

3.2 Implementation of Replications

?? The following replications are modelled after surveys of the phenomenology of psychedelic states (Preller and Vollenweider 2016; Kometer and Vollenweider 2016) and personal reports (Kleinman, Gillin, and Wyatt 1977).

3.2.1 Spatial Effects

The spacial effects of this section are a form of a vertex shader, or part thereof. UE4 has a concept of so-called “materials” – assets that can be applied to meshes to control the visual look of 3D assets. UE4 materials are defined using a built-in visual programming node graph. While this approach of specifying graphics processing unit (GPU) shader logic allows for tighter integration with UE4’s rendering engine and its lighting model, it makes it difficult to use conventional shading languages such as OpenGL Shading Language (GLSL) or High Level Shading Language (HLSL). The usage of conventional shading languages is sometimes desirable, because the provided material node graph editor cannot, by design, express some control flow constructs, such as loops.

However unwieldy, it is possible to use HLSL code in material graphs, in UE4. The directory of our custom HLSL shader files must be properly registered in the engine via an engine plugin (Alessa Baker 2021). The shader files can then be referenced from within “custom” nodes of the material node graph editor.

3.2.1.1 Depth Perception Distortion

This replication simulates the distorted perception of depth, micropsia, and macropsia (Fischer et al. 1970; Dittrich 1998; Hill, Fischer, and Warshay 1969; Hill and Fischer 1973).

Our replication of the depth perception distortion is implemented as a world-space vertex shader. Even though certain distortions in screen-space may also result in the distortion of depth perception, we chose our approach to achieve better control over the shape of the rendered geometry.

⁴Released by Greg Zaal under the CC0 1.0 (public domain) license.

⁵<https://web.archive.org/web/20220515010919/https://polyhaven.com/a/cannon>

3.2.1.1.1 First Attempt Our first attempt made use of a self-similar, bijective and continuous function f to modify the distance of vertices from the **HMD**. The self-similarity is required to ensure that no self-intersection of geometry occurs, after the offset has been applied.

$$f(r) = a^{\frac{1}{\pi} \sin(\pi \log_a r) + \log_a r} \quad (3.1)$$

Where $a \in (1; +\infty)$.

The interesting property of self-similarity results in the maximum offset being directly proportional to the distance of the **HMD**. The graph of the function can be seen in figure 3.3.

Figure 3.3: First attempt at distorting depth perception, unused in the final application. The function f from equation 3.1 modifies the distance of vertices from the **HMD**. Parameter $a = 1.5$.

Although this first iteration resulted in visually enticing results, we also noticed that it caused motion sickness in **VR**, particularly during the user's movement. We believe the motion sickness was caused by clusters of geometry moving with the position of the **HMD**, as if attracted to it, and caused a discrepancy between the user's vestibular system and the visual information.

Another disadvantage of this solution is its predictability and the synthetic look caused by its uniformity.

3.2.1.1.2 Final Solution In order to break up clusters of similarly affected geometry, we decided to use procedural noise. Procedural noise has been used for the generation of textures (Perlin 1985), and would be suitable to create a less predictable, more chaotic effect.

There are various kinds of procedural noise used in computer graphics. We found Simplex noise (Olano et al. 2002) to be suitable for our use-case, particularly for its $\mathcal{O}(n^2)$ time complexity in n dimensions, lack of directional artifacts (visual isotropy), and a well-defined continuous gradient.

Let's denote the simplex noise sampling function as $s: \mathbb{R}^n \rightarrow \mathbb{R}$.

Now that we have a way to sample the noise, we could try to use the noise sample (possibly scaled by a constant) as the offset of the distance of each vertex to the **HMD**, as shown in the previous section. To retrieve the sample, we can use:

$$s' := s \left(\begin{bmatrix} f_s x \\ f_s y \\ f_s z \\ f_t t \end{bmatrix} \right) \quad (3.2)$$

where s' is the resulting sample, x , y and z are spacial coordinates of any point in space (typically the position of a vertex), t is the current time in seconds, and f_s and f_t are space-wise and time-wise frequencies of the noise, respectively.

With the addition of the time coordinate, resulting in 4-dimensional noise, the sampled offset value will change over time. This helps break up the uniformity and predictability of the previous solution.

Unfortunately, we have lost one important property of the previous solution: The fact that the maximum offset was directly proportional to the distance from the **HMD**. We could try to reintroduce proportionality naively by multiplying the sample by the distance r :

$$s' := r \cdot s \begin{pmatrix} f_s x \\ f_s y \\ f_s z \\ f_t t \end{pmatrix} \quad (3.3)$$

By this modification, we have effectively changed the amplitude of the noise, yet the frequency remains the same – and uniform. If we were to use this sample s' as the distance offset, we would cause distant geometry to self-intersect. Therefore, a different solution is needed.

For this task, we may use fractional Brownian motion (**fBm**). Before we go into how **fBm** can help resolve this issue, let's briefly describe how it is used in the synthesis of self-similar noise. **fBm** is a technique of combining layers of noise, while varying their amplitudes and frequencies.

$$s' := \frac{1}{k} \sum_{i=0}^{k-1} g^i \cdot s \left(l^i \begin{bmatrix} f_s x \\ f_s y \\ f_s z \\ f_t t \end{bmatrix} + i \vec{o} \right) \quad (3.4)$$

In equation 3.4, we combine $k \in \mathbb{N}$ layers of simplex noise. The parameter $g \in \mathbb{R}$ (gain) changes the amplitude of each layer, and the parameter $l \in \mathbb{R}$ (lacunarity) changes the frequency of each layer. Typically, $l = \frac{1}{g}$; in that case, we are generating so-called “pink noise”. The parameter $\vec{o} \in \mathbb{R}^n$ is a coordinate offset applied to each layer, to break up symmetry (a different seed for each layer could also be used).

Now, back to our original problem of keeping the amplitude proportional to the distance from the **HMD**. Instead of using k layers of noise with indices $i = 0, 1, \dots, k - 1$, we can offset the indices by an integer value depending on the distance from the **HMD**. If we do so carefully, we will recover the direct proportionality. We define a real-valued offset $m: \mathbb{R} \rightarrow \mathbb{R}$:

$$m(r) = \log_a r \quad (3.5)$$

Where $a \in \mathbb{R}$ is a parameter; more on this later. Then, we can define the rounded-down integer part $j: \mathbb{R} \rightarrow \mathbb{Z}$ to offset the layer indices with:

$$j(r) = \lfloor m(r) \rfloor \quad (3.6)$$

$$s' := \frac{1}{k} \sum_{i=0}^{k-1} g^{i+j(r)} \cdot s \left(l^{i+j(r)} \begin{bmatrix} f_s x \\ f_s y \\ f_s z \\ f_t t \end{bmatrix} + (i + j(r)) \vec{o} \right) \quad (3.7)$$

Equation 3.7 differs from equation 3.4 in that we have added an index offset $j(r)$, which is computed from the distance to the **HMD** r . Now we are able to offset the indices. However, this will result in noticeable discontinuities of the noise at the discontinuities of $j(r)$.

In order to remove these discontinuities, we shall introduce blending. Let us refer to the layers at indices $j(r), j(r) + 1, \dots, j(r) + k - 1$ as “active layers”, the layer at index $j(r)$ as “the first active layer” and the layer at index $j(r) + k - 1$ as “the last active layer”.

Let us define a weight function $w: \mathbb{Z} \times \mathbb{R} \rightarrow [0; 1]$, which will attenuate the first and last active layer, while leaving other layers unaffected.

$$w(i, r) = \begin{cases} m(r) - j(r) = \{m(r)\} & \text{if } i = 0 \\ 1 - (m(r) - j(r)) = 1 - \{m(r)\} & \text{if } i = k \\ 1 & \text{otherwise} \end{cases} \quad (3.8)$$

Where $\{x\} = x - \lfloor x \rfloor$ is the upper fractional part of x .

$$s' := \frac{1}{k} \sum_{i=0}^k w(i, r) \cdot g^{i+j(r)} \cdot s \left(l^{i+j(r)} \begin{bmatrix} f_s x \\ f_s y \\ f_s z \\ f_t t \end{bmatrix} + (i + j(r)) \vec{o} \right) \quad (3.9)$$

Besides multiplying each layer by the weight $w(i, r)$, we have also changed the upper index of the sum from $k - 1$ to k , to account for the attenuation.

We have arrived at the derived general equation for blended **fBm** noise based on distance r with parameters $a, g, l \in \mathbb{R}; \vec{o} \in \mathbb{R}^n; k \in \mathbb{N}$. However, in general, this form does not satisfy our requirement of the amplitude being proportional to the distance r . In order for that to be true, we must set $a = g = \frac{1}{l}$.

The equation then expands to:

$$s' := \frac{1}{k} \sum_{i=0}^k w(i, r) \cdot a^{i+\lfloor \log_a r \rfloor} \cdot s \left(a^{-(i+\lfloor \log_a r \rfloor)} \begin{bmatrix} f_s x \\ f_s y \\ f_s z \\ f_t t \end{bmatrix} + (i + \lfloor \log_a r \rfloor) \vec{o} \right) \quad (3.10)$$

$$w(i, r) = \begin{cases} \{\log_a r\} & \text{if } i = 0 \\ 1 - \{\log_a r\} & \text{if } i = k \\ 1 & \text{otherwise} \end{cases} \quad (3.11)$$

Finally, we may or may not want the frequency of the fourth coordinate to be influenced by lacunarity. We reached better results when lacunarity did not affect the time coordinate.

$$s' := \frac{1}{k} \sum_{i=0}^k w(i, r) \cdot a^{i + \lfloor \log_a r \rfloor} \cdot s \left(\begin{bmatrix} a^{-(i + \lfloor \log_a r \rfloor)} f_s x \\ a^{-(i + \lfloor \log_a r \rfloor)} f_s y \\ a^{-(i + \lfloor \log_a r \rfloor)} f_s z \\ f_t t \end{bmatrix} + (i + \lfloor \log_a r \rfloor) \vec{o} \right) \quad (3.12)$$

This is the final equation used to sample blended **fBm** noise based on the distance r with parameters $a \in \mathbb{R}, \vec{o} \in \mathbb{R}^n, k \in \mathbb{N}$. This equation is used in the application to displace vertices of scene geometry. The result is scaled to ensure that no self-intersections of scene geometry occur.

Figure 3.6: Computation of active layers based on the distance from the **HMD**. Active layers as solid black lines. Green areas correspond to the weight of the first and last currently active layer.

Figure 3.7: Amplitudes of active layers based on the distance from the **HMD**, for the case where $a = g = 1.5$. Active layers as solid black lines. The green line shows the direct proportionality of the maximum active layer amplitude and the distance from the **HMD**.

3.2.1.2 Visual Drifting

In this section, we describe the implementation of our replication of visual drifting, sometimes described as the “breathing” or “morphing” of objects (Díaz 2010; Kleinman, Gillin, and Wyatt 1977).

As with depth perception distortion, there are two ways of implementing this replication, depending on the coordinate system and stage of rendering affected – world-space and screen-space.

Ideally, the realism of the final implementation should not be broken by:

1. the rotation of the **HMD**;
2. the movement of the **HMD** up to regular walking speed;
3. the fast movement of objects in the scene.

We chose to avoid a screen-space implementation, because satisfying any of those requirements seemed very difficult. Nevertheless, we are confident that our world-space solution satisfies at least the first two of the requirements.

We can use procedural noise to offset vertices into arbitrary directions in 3 dimensional space, but we need to be careful so that we do not cause geometry to self-intersect. Thankfully, we have already solved this problem in the previous section, and we can use that noise function.

Let us consider the general equation 3.9 with $a = g = \frac{1}{l}$, and denote the right-hand side expression as a vector field $S: \mathbb{R}^n \rightarrow \mathbb{R}$, where $n = 4$:

$$S\left(\begin{bmatrix} x \\ y \\ z \\ t \end{bmatrix}\right) = \frac{1}{k} \sum_{i=0}^k w(i, r) \cdot g^{i+j(r)} \cdot s\left(l^{i+j(r)} \begin{bmatrix} f_s x \\ f_s y \\ f_s z \\ f_t t \end{bmatrix} + (i + j(r))\vec{o}\right) \quad (3.13)$$

Then, we have two ways of using this noise function to generate an offset vector $\vec{v} \in \mathbb{R}^3$.

Option one.

We compose the offset vector \vec{v} from three samples of S with coordinate offset vectors $\vec{o}_0, \vec{o}_1, \vec{o}_2 \in \mathbb{R}^4$ to ensure different samples (different seeds would also work).

$$\vec{v} := \left[S\left(\begin{bmatrix} x \\ y \\ z \\ t \end{bmatrix} + \vec{o}_0\right) \quad S\left(\begin{bmatrix} x \\ y \\ z \\ t \end{bmatrix} + \vec{o}_1\right) \quad S\left(\begin{bmatrix} x \\ y \\ z \\ t \end{bmatrix} + \vec{o}_2\right) \right]^T \quad (3.14)$$

Option two.

We use the first 3 components of the gradient of S as the offset vector \vec{v} .

$$\vec{v} := \begin{bmatrix} 1 & 0 & 0 & 0 \\ 0 & 1 & 0 & 0 \\ 0 & 0 & 1 & 0 \end{bmatrix} \nabla S\left(\begin{bmatrix} x \\ y \\ z \\ t \end{bmatrix}\right) \quad (3.15)$$

The second option seems much more elegant, does not require 3 samples, and may even yield nicer results. Option two was our choice.

Unfortunately, the distance from the **HMD** r is dependent on the x, y and z coordinates, which makes the gradient overly complex. For that reason, we have decided to simplify the gradient by treating the r parameter as a constant. We shall denote this simplification of the gradient ∇S as $S_G: \mathbb{R}^n \rightarrow \mathbb{R}^n$.

$$S_G\left(\begin{bmatrix} x \\ y \\ z \\ t \end{bmatrix}\right) = \frac{1}{k} \sum_{i=0}^k w(i, r) g^{i+j(r)} \nabla s\left(l^{i+j(r)} \begin{bmatrix} f_s x \\ f_s y \\ f_s z \\ f_t t \end{bmatrix} + (i + j(r))\vec{o}\right) \odot \begin{bmatrix} f_s \\ f_s \\ f_s \\ f_t \end{bmatrix} l^{i+j(r)} \quad (3.16)$$

$$= \begin{bmatrix} f_s \\ f_s \\ f_s \\ f_t \end{bmatrix} \odot \left(\frac{1}{k} \sum_{i=0}^k w(i, r) g^{i+j(r)} \nabla s\left(l^{i+j(r)} \begin{bmatrix} f_s x \\ f_s y \\ f_s z \\ f_t t \end{bmatrix} + (i + j(r))\vec{o}\right) l^{i+j(r)} \right) \quad (3.17)$$

The \odot operator is the component-wise vector multiplication. For $g = \frac{1}{l}$, we could simplify further:

$$S_G \left(\begin{bmatrix} x \\ y \\ z \\ t \end{bmatrix} \right) = \begin{bmatrix} f_s \\ f_s \\ f_s \\ f_t \end{bmatrix} \odot \left(\frac{1}{k} \sum_{i=0}^k w(i, r) \nabla_s \left(l^{i+j(r)} \begin{bmatrix} f_s x \\ f_s y \\ f_s z \\ f_t t \end{bmatrix} + (i + j(r)) \vec{o} \right) \right) \quad (3.18)$$

As we can see in figure 3.8, the direct proportionality of the amplitude and the distance r has been lost. We could have also noticed the $g^{i+j(r)}$ term being cancelled during the simplification step to equation 3.18. In order to recover it, we need to divide the right-hand side of equation 3.17 by $l^{i+j(r)}$.

$$S'_G \left(\begin{bmatrix} x \\ y \\ z \\ t \end{bmatrix} \right) = \begin{bmatrix} f_s \\ f_s \\ f_s \\ f_t \end{bmatrix} \odot \left(\frac{1}{k} \sum_{i=0}^k w(i, r) g^{i+j(r)} \nabla_s \left(l^{i+j(r)} \begin{bmatrix} f_s x \\ f_s y \\ f_s z \\ f_t t \end{bmatrix} + (i + j(r)) \vec{o} \right) \right) \quad (3.19)$$

We denote this modulated version of the simplified gradient as S'_G . As seen in figure 3.9, the proportionality is recovered.

This is the final function we have used in our application to displace vertices of the scene geometry. To recapitulate the requirements we have placed upon ourselves to implement this replication, we required the realism not to be broken by the following actions.

- ☒ The rotation of the **HMD**. Does not influence the sampling in any way, only the location of the **HMD** is relevant. Success.
- ☒ The movement of the **HMD** up to regular walking speed. The movement of the **HMD** makes objects shift their active layers in a continuous, smooth way. Success.
- ☐ The fast movement of objects in the scene. Objects moving fast across the screen(s) might appear to morph erratically, significantly faster than the animation speed of still objects. Not ideal.

Regarding the last point, one might think to modulate the vertex offset by the object's inverse velocity to account for the erratic animation, however, that might result in the object intersecting with the rest of the scene – for example, with a static wall unaffected by the modulation.

We did not expect any fast-moving objects in the scene, and so this implementation was sufficient for our application.

3.2.2 Non-Spatial Effects

The following replications are implemented entirely as screen-space post-processing effects, that is, applied to the 2-dimensional texture which results from rendering the 3-dimensional scene. **VR HMDs** typically make use of multiple screens for stereoscopic rendering. The post-processing effects are applied to all of the textures corresponding to each screen in the **HMD**.

While UE4 does provide a way to create post-processing effects via “post process materials”, these assets are limited by the design of the rendering engine and the lighting model. For example, it is not possible to define custom framebuffers for use in temporal post-processing effects.

Such features require the modification of the rendering dependency graph (RDG), UE4 graph-based abstraction designed to perform whole-frame optimization of the rendering pipeline. At the same time, the documentation of this feature is very limited, with the most reliable resources being the engine’s code itself, and various blog posts on the internet.

Thankfully, we could make use of a boiler-plate example plugin (Ossi Luoto 2021) that showcases interaction with the RDG, which we modified for our purposes.

3.2.2.1 Visual Acuity Enhancement

Classical hallucinogens are known to cause alterations in the perception of elementary visual features, such as brightness, color saturation, and visual contrast (Heinrich Klüver 1942; Klüver 1966; Dittrich 1998; Díaz 2010; Siegel and Jarvik 1975; Fischer, Hill, and Warshay 1969), as well as in the perception of detail in the textures of objects (PsychonautWiki 2020). This may contribute to the sense of novelty typical during classical hallucinogen-induced ASCs.

3.2.2.1.1 Enhancement of Saturation and Contrast The implementation of the enhancement of saturation and contrast is done entirely with the use of in-engine features of UE4. UE4 makes it possible to define a global post-processing volume (a volume spanning the entirety of the scene), that applies select basic post-processing effects to the rendered views. These effects include modifiers for the saturation and contrast of the rendered views.

Besides saturation and contrast, a modifier for brightness is also available, although we did not end up using it, because the dynamic range of our VR headset (the *HTC Vive* and the *HTC Vive Pro*) was not sufficient to make proper use of the effect.

3.2.2.1.2 Enhancement of Texture Detail via Sharpening In order to increase the apparent texture detail globally, we used a sharpening post-processing effect. Sharpening results in the enhancement of local contrast, or the enhancement of high-frequency information of the modified image.

We decided to use the well known unsharp masking algorithm (Jain 1989), with Gaussian blur as the low-pass filter, for our implementation of the sharpening filter. A possible form of the unsharp masking expression, that we made use of, is

$$\vec{c}' := \vec{c} + i \cdot (\vec{c} - \vec{c}_{G(r)}) \quad (3.20)$$

where $\vec{c}' \in [0; 1]^3$ is the resulting texel color, $\vec{c} \in [0; 1]^3$ is the original texel color, $\vec{c}_{G(r)} \in [0; 1]^3$ is the color of the texel at the same position in the source texture with a Gaussian blur of radius $r \in [0; +\infty)$ applied to it, and $i \in \mathbb{R}$ is the intensity of the effect.

Since Gaussian blur is a low-pass filter, the result of $(\vec{c} - \vec{c}_{G(r)})$ is a high-pass filtered image, as it is the original without the low-frequency information.

A 2-dimensional Gaussian blur may be implemented in two ways; via a 2-dimensional convolution, or, thanks to the Gaussian blur being a separable filter, using a two-pass 1-dimensional convolution. The time complexity is $\mathcal{O}(w_{kernel}^2 w_{image} h_{image})$ and $\mathcal{O}(w_{kernel} w_{image} h_{image})$, respectively.

We used the two-pass 1-dimensional method for its advantageous time complexity. Our implementation pre-computes one half of the symmetric convolution matrix on the CPU, according to the specified radius and the resolution of the texture. The execution order of separate steps of the algorithm is shown in figure 3.10.

The resulting sharpening effect (without uniform saturation and contrast enhancement from the previous section) can be seen in figure ??.

It is noteworthy to mention one significant drawback of our approach – the resulting effect is not perceptually uniform across the whole screen. This is caused by the fact that we see the majority of the screen under an non-perpendicular angle, and so the convolution matrix is skewed from our point of view. As an improvement for the future, one might want to consider performing the Gaussian blur on the surface of a sphere centered around the HMD, to which the screen texture is projected.

Figure 3.10: Execution order of distinct components of the sharpening effect.

3.2.2.2 Tracers

“Tracers” is the colloquial name for visual tracing, the last aspect of psychedelic-induced ASCs we implemented a replication of in our application. Tracers are shown as positive after-images of moving objects, and can appear either continuous or discontinuous (Hartman and Hollister 1963; Díaz 2010; Anderson and O’Malley 1972; Kleinman, Gillin, and Wyatt 1977). We focused on the replication of the continuous form of tracers.

The implementation required the persistence of image data between frames, which has been accomplished by the usage of an accumulation texture, one for each screen of the HMD. The replication has been implemented via the following post-processing operation:

$$\vec{c}' := \text{lerp}(\vec{c}, \vec{a}, \beta^{\Delta t} \cdot \alpha) \quad (3.21)$$

$$\vec{a}' := \text{lerp}(\vec{c}, \vec{a}, \beta^{\Delta t}) \quad (3.22)$$

where

$$\text{lerp}(x, y, t) = (1 - t)x + ty \quad (3.23)$$

is the the linear interpolation function, also known as `mix` in GLSL and `lerp` in HLSL, $\vec{c} \in [0; 1]^3$ is the original color of the texel from the source texture, $\vec{c}' \in [0; 1]^3$ is the modified color of the texel stored in the output texture, $\vec{a} \in [0; 1]^3$ is the original color of the texel from the accumulation texture, $\vec{a}' \in [0; 1]^3$ is the modified color of the texel stored in the accumulation texture, $\Delta t \in [0; +\infty)$ is the duration since the previous frame, and $\alpha, \beta \in [0; 1]$ are parameters.

Another visualization of the operation is shown as an execution graph in figure 3.11.

The parameter α corresponds to the overall opacity of the effect, which is fine-tuned, so that the effect does not cause motion sickness by dominating the visual field. The

parameter β controls the feedback strength, which can be understood as a parameter that influences the duration of the temporal blur or “exposition time”. The Δt parameter provides resiliency to framerate fluctuations.

This is the final form of the effect that has been used in our application.

Nevertheless, the current form of the implementation has some drawbacks, that we have identified late in the development of the application.

First, we have received feedback, that the tracers should not be as noticeable during the movement or rotation of the **HMD**, compared to moving objects in the scene. Despite that, we decided to keep our implementation, because we find it unlikely, that the psychedelic-induced **ASC** would somehow change the perception of objects moving relative to some kind of absolute world frame *only*, rather than of any object that has been moved within the person’s field of view.

And second, our implementation completely ignores the direction the user is looking, it only considers the rotation of the **HMD**. A precise eye-tracking device built-into the **HMD** would be required to develop a method that takes the the direction of eyes into account.

Finally, regarding discontinuous tracers, the implementation of such an effect would require keeping more temporal information than just a single accumulation texture. Probably, a 3-dimensional texture would have to be used, with the width and height of the screen and the depth of $\frac{1}{\Delta t} \cdot T$, where $\frac{1}{\Delta t}$ is the framerate, and $T \in (0; +\infty)$ is the delay of the first positive after-image of the tracers. The main challenges may stem from the fact that the framerate of a **VR** application is typically not uniform, as well as from the memory requirements for storing such texture.

Figure 3.11: Execution graph of the tracer effect. The parameter $\alpha \in [0; 1]$ is the total opacity of the effect. The parameter $\beta \in [0; 1]$ is the feedback modifier corresponding to the “duration” of the resulting blur. Finally, $\Delta t \in [0; +\infty)$ is the time since the previous frame, making the effect less influenced by framerate fluctuations. The accumulation texture is first read from, then written to.

Figure 3.12: The tracer effect is applied in the second render pass of the sharpening effect.

3.3 Complex Replication

The complex replication, which is supposed to simulate a significant portion of an **ASC** induced by classical psychedelics, is the combination of the partial replications described in section ??.

3.3.1 Execution Order

The task of combining partial replications raises the question, in which order they should be arranged. First, we must acknowledge, that there are requirements on the order of the replications, based on their position in the rendering pipeline of **UE4**. For example, spatial effects affecting the position of vertices of the scene geometry are a part of the vertex shader, and therefore precede non-spatial, post-processing effects. At the same

time, we cannot influence the order of the *saturation and contrast enhancement*, as it uses the engine’s built-in post-processing pass. Thankfully, the order of this particular effect among other post-processing effects would have no influence on the resulting image anyway. Thus, we are left with the following decisions on the relative order of the following replications.

We have two possible orderings for the spatial effects.

1. Depth Perception Distortion → Visual Drifting
2. Visual Drifting → Depth Perception Distortion

We certainly do not want the *visual drifting* to be applied after the *depth perception distortion*, as that would mean the sampling coordinates of vertices of static geometry would change and have a significantly visible impact on the resulting effect. Therefore, we chose option 2.

Next, we need to consider the ordering of the remaining two non-spatial, post-processing effects.

1. Enhancement of Texture Detail via Sharpening → Tracers
2. Tracers → Enhancement of Texture Detail via Sharpening

We do not want the tracers to be sharpened, as the goal of sharpening was to enhance the detail of textures. Additionally, sharpening the tracers might reveal the discrete implementation of the color accumulation into the accumulation buffer, which may become visible particularly for moving objects, or during the movement of the **HMD**. Therefore, we chose option 1.

The complete order of all of the effects, as implemented in our application, is shown in figure 3.13.

Figure 3.13: The execution order of partial replications, making up the complex replication.

3.3.2 Experiment Automation and Controls

In order to make the application behave in a reproducible way, for testing, we had to automate it. Our study, as discussed in chapter 4, required an active scenario and a control scenario. The only difference between these scenarios is the influence of the overall complex replication.

For the control scenario, the complex replication is completely disabled, for the whole duration of the test. In respect for the participants of our study, we wanted to keep the tests short mainly because of the control scenario, where the participants would have to keep the **HMD** on, while nothing interesting was happening in the application. Each scenario was therefore decided to last 10 minutes.

For the active scenario, the influence of the complex replication is controlled via a *master influence* variable, the value of which is changed throughout the test, according to a function loosely modelled after the stages of a psychedelic experience from figure 2.1, or the typical plasma concentration-time profile of the psychedelic. We modified the function, so that the drop-off is not as steep and lasts longer, otherwise the user would not be able to experience the effects at a high influence for enough time, since the “peak” lasts only

about 1-2 minutes. The resulting function of the *master influence* variable is shown in figure 3.14.

We also added informational messages to indicate the beginning and end of the test, displayed in front of the participant in the virtual scene.

Each scenario can be launched with a key combination:

- Control: Shift-C
- Active: Shift-T

This way, the administrator can launch the appropriate scenario and focus their attention on keeping the participant safe from, e.g., tripping over the HMD's cable or hitting a wall.

Figure 3.14: TODO

(a)
Sim-
plex
noise
from
eq.
3.2.

(b)
Sim-
plex
noise
fBm
from
eq.
3.4,
with
co-
or-
di-
nate
off-
set
 $\vec{o} =$
 $\vec{0}$
and
pa-
ram-
e-
ters
 $g =$
 $\frac{1}{l} =$
1.5, $k =$
5.

(c)
Sim-
plex
noise
fBm
from
eq.
3.4,
with
non-
zero
co-
or-
di-
nate
off-
set
 $\vec{o} \neq$
 $\vec{0}$
and
pa-
ram-
e-
ters
 $g =$
 $\frac{1}{l} =$
1.5, $k =$
5.

(d)
Sim-
plex
noise
fBm
with
in-
dex
off-
sets
based
on
the
dis-
tance
to
the
cen-
ter
 r ,
from
eq.
3.7,
with
non-
zero
co-
or-
di-
nate
off-
set
 $\vec{o} \neq$
 $\vec{0}$
and
pa-
ram-
e-
ters
 $a =$
 $g =$
 $\frac{1}{l} =$

Figure 3.5: The final implementation of the blended **fBm** Simplex noise based on the distance to the center r , from eq. 3.12, with non-zero coordinate offset $\vec{o} \neq \vec{0}$ and parameters $a = g = \frac{1}{l} = 1.5, k = 5$. Amplitude adjusted for visualization.

Figure 3.8: The first 3 components of the simplified gradient of the blended **fBm** simplex noise S_G , from eq. 3.18, with non-zero coordinate offset $\vec{o} \neq \vec{0}$ and parameters $a = g = \frac{1}{l} = 1.5, k = 5$. Components visualized as channels of the additive RGB color space. Amplitude adjusted for visualization and clipped to range.

Figure 3.9: The first 3 components of the simplified gradient of the blended **fBm** simplex noise S'_G , from eq. 3.19, with non-zero coordinate offset $\vec{o} \neq \vec{0}$ and parameters $a = g = \frac{1}{l} = 1.5, k = 5$. Components visualized as channels of the additive RGB color space. Amplitude adjusted for visualization and clipped to range.

4 | Evaluation

4.1 Methods

We propose the following hypotheses to investigate whether the implemented complex replication has any effect on the scores of the **5D-ASC** and **11-ASC** scorings.

- Null hypothesis H_0 : The implemented complex replication **does not have any effect** on the scores of the **5D-ASC** and **11-ASC** scorings.
- Alternative hypothesis H_1 : The implemented complex replication **does have an effect** on the scores of the **5D-ASC** scoring, the **11-ASC** scoring, or both.

A controlled within-subject study including $N = 10$ participants, was conducted to test these hypotheses, with a statistical significance level of $\alpha = 0.05$.

The following demographic statistics are known about the population:

- Age: mean of 30 years, standard deviation of 10.1 years.
- Gender: 5 male, 4 female, 1 non-binary.

The requirements for participation in the study, inspired by Bartossek, Kemmerer, and Schmidt (2021), were as follows:

- No alcohol use in the past 12 hours prior to the session.
- No **THC** use in the past week prior to the session and no more than twice a week in the last year.
- No use of psychedelic substances in the last two weeks prior to the session.
- Not pregnant.
- 18 years or older.

The participants were required to reserve two sessions, each on a different day, for the active and control scenarios, the order of which was chosen at random. 5 out of 10 participants underwent the control scenario on their first session.

The first session consisted of:

1. An explanation of the study and the procedure of the session.
2. Signing of the informed consent form (see appendix B).
3. Testing of the developed VR application for 10 minutes, with either the control or the test scenario.
4. Filling out of the psychometric questionnaire.

The second session consisted of:

1. Testing of the developed VR application for 10 minutes, with the remaining scenario.
2. Filling out of the psychometric questionnaire.

The study was conducted with the following hardware specifications.

HMD	HTC Vive Pro
Tracking	2 SteamVR Base Stations 2.0
CPU	Intel® Core™ i9-10900X
GPU	NVIDIA® GeForce® RTX 2080 Ti
RAM Capacity	128 GB

Figure 4.1: Resulting scores according to the 5D-ASC scoring for control and test scenarios. Error bars show the 95% confidence interval of the true mean, assuming normal distribution. Statistical significance indicated with * ($p < 0.05$) and *** ($p < 0.001$).

Figure 4.2: Resulting scores according to the 11-ASC scoring for control and test scenarios. Error bars show the 95% confidence interval of the true mean, assuming normal distribution. Statistical significance indicated with * ($p < 0.05$).

4.2 Results

With the assumption that the individual factors of each of the scorings are normally distributed, we used the repeated measures *paired t-test* to test our hypotheses. Most recent studies utilizing the 5D-ASC and the 11-ASC scorings assume the resulting factors to be normally distributed, and so do we. For alternatives, see appendix C.

The results of the 5D-ASC scorings, shown in figure 4.1, indicate a significant difference for the “Dread of Ego Dissolution” ($p = 0.0204 < 0.05$) and “Vigilance Reduction” ($p = 9.16 \cdot 10^{-6} < 0.001$) dimensions.

The results of the 11-ASC scorings can be seen in figure 4.2, and indicate a significant difference for the “Disembodiment” ($p = 0.0357 < 0.05$) and “Anxiety” ($p = 0.0387 < 0.05$) factors.

Based on these results, we reject the null hypothesis H_0 , that “the implemented complex replication does not have any effect on the scores of the 5D-ASC and 11-ASC scorings.”

5 | Conclusion

5.1 Discussion

In this work, we have explored various contemporary attempts at replicating altered states of consciousness (ASCs) induced by classical psychedelics. We have also explored potential applications of the replications of psychedelic-induced ASCs.

We created an application for immersive virtual reality (VR), which is capable of producing a complex replication of a psychedelic-induced ASC. This complex replication was a combination of partial replications of the following distinct aspects typical for a low-dose “perceptual stage” psychedelic-induced ASCs:

1. Depth Perception Distortion
2. Visual Drifting
3. Visual Acuity Enhancement
4. Tracers (Visual Tracing)

We measured the impact of the implemented complex replication with $N = 10$ subjects on the scores of the 5-Dimensional Altered States of Consciousness Questionnaire (5D-ASC) and the 11-Factor Altered States of Consciousness Questionnaire (11-ASC), and confirmed, that they are influenced by the implemented complex replication. This finding suggests, that VR is an effective medium for the replication of certain aspects of ASCs.

5.2 Limitations

The study we have conducted was constrained by the following limitations.

Lack of the Visualization of the User’s Body

Displaying the user’s body in VR realistically is an unsolved issue for consumer-grade VR systems. Ideally, the user would be able to see their real body, possibly via a filtered view of a pass-through camera built-into the head-mounted display (HMD), or maybe via a 3D-reconstructed model from external cameras. A 3D-reconstructed model would be ideal, because the spatial effects could be applied to the scene as well as the body, which would provide an better sense of micropsia and macropsia.

Low Sample Size

The results of our study were mainly limited by the low number of participants ($N = 10$). We might have been able to reach more conclusive results, had the sample size been larger.

No Sound Isolation

Our experimental conditions did not allow for sound isolation. Often, noises could be heard from adjacent rooms, or from the outside through the window that we consistently kept open during testing. In retrospect, a closed room with proper sound isolation and a quiet ventilation system would have provided better experimental conditions. The silence could be substituted with natural ambient noises appropriate for the virtual scene.

5.3 Future Work

Other Replications

Our work has definitely not exhausted all aspects of psychedelic-induced ASCs for the replication via VR. The following aspects come to mind, that we think would be suitable for VR. The main challenge is to be able to implement the replications in a general way, so that they perform well no matter the virtual scene the user finds themselves in.

Time Perception Distortion

By distorting the simulation timestep, we might be able to replicate the sense of distorted time perception. The virtual scene of our application did not have any elements or objects for which that would matter, and so we could not simulate this effect.

Synesthesiae

The replication of various kinds of synesthesia could be explored; mainly, audio-visual synesthesia, or audio-vibrotactile synesthesia. We did not attempt to replicate these kinds of synesthesia, as they would require sound, which our application lacks. Both of these synesthesiae would provide the best experience with music; however, music tends to have a significant emotional impact on the listener, that might have distorted the measurements in our study, and so no music was used.

Auditory Effects

Various kinds of auditory distortions could be explored. Specifically, slight variations in pitch and speed of playback seem like potential effects suitable for replication.

Discontinuous Visual Tracing

We have implemented a continuous form of visual tracing and hinted towards a possible method of implementing a discontinuous form visual tracing.

Hue Shifting

A common effect of classical psychedelics are various forms of hue shifting. We avoided this aspect, as we did not feel confident in replicating it correctly. A thorough examination of individual reports of psychedelic experiences, which detail this phenomenon, may be in order.

A Stronger Hypothesis

In this work, we only measured whether the implemented replication had any effect on the questionnaire scorings. A stronger hypothesis would be to model a specific psychedelic substance and attempt to match the results of the questionnaire scorings with results from a low-dose clinical study of that substance. However, this would require, comparatively, a massive amount of effort.

Eye Tracking

Eye tracking has the potential not only to improve the performance of our application using state of the art rendering technologies, such as foveated rendering, it also has the potential to improve the implementation of our replication of *visual tracing*. Currently, our implementation of this replication responds to the movement of the **HMD**, rather than the movement of eyes.

Hand Tracking

As discussed in the limitations, our application lacks a representation of the user's body. We proposed a solution by modelling the user's entire body, but there is also a possible middle ground that could be pursued instead – tracking the user's hands. The user's virtual representation of their hands may be sufficient to provide a better sense of spatial effects.

An Indoor Scene

Our application uses an outdoor scene, but the complex replication is implemented in a universal way, such that it can be used in any scene, including an indoor scene. An indoor scene might result in vastly different scores of the chosen questionnaire scorings.

Geometry Subdivision

The implemented spatial effects could be improved by the use of dynamic subdivision of geometry. Both spatial effects make use of a non-linear transformation of vertices. This results in the movement of seams of any two intersecting models. Dynamic subdivision may be used to mitigate this issue, by making it less apparent.

Unfortunately, dynamic subdivision requires geometry shaders, which are considered deprecated, in the current version of graphics application programming interfaces (**APIs**). Fortunately, they have been deprecated in favor of mesh shaders. Nevertheless, the implementation of dynamic subdivision in **UE4** has been unreliable.

List of Acronyms

- 11-ASC** 11-Factor Altered States of Consciousness Questionnaire: A version of the *Altered States of Consciousness Rating Scale* psychometric questionnaire, which is based on the hypothesis that **ASCs** have a common core independent of the induction method which distinguishes them from the waking conscious state (Figueiredo et al. 2016; Studerus, Gamma, and Vollenweider 2010).
- 5-HT** 5-hydroxytryptamine, also known as serotonin
- 5D-ASC** 5-Dimensional Altered States of Consciousness Questionnaire: Like the **11-ASC**, but with different scoring and categories (Dittrich, Lamparter, and Maurer 2010).
- AI** artificial intelligence
- API** application programming interface
- ASC** altered state of consciousness: See section 2.1 for a complete definition and related terms.
- CPU** central processing unit
- DCNN** deep convolutional neural networks
- DMT** *N,N*-dimethyltryptamine: A classical hallucinogenic drug first synthesized in 1931 (Manske 1931), a psychoactive compound of Ayahuasca, the ceremonial spiritual medicine used by Amazonian natives for shamanic purposes and to bond socially in a casual setting (Mark Hay 2020).
- DSP** digital signal processing
- EEG** electroencephalograph
- FOV** field of view
- FPS** frames per second: A unit of monitor refresh rate, equivalent to hertz (Hz).
- GLSL** OpenGL Shading Language: A shading language used by the OpenGL graphics **API**.
- GPU** graphics processing unit: A specialized extension module providing acceleration for computer graphics computations and other parallelizable tasks.
- HDRI** high dynamic range imaging
- HLSL** High Level Shading Language: A shading language used by the DirectX graphics **API**.
- HMD** head-mounted display

LSD lysergic acid diethylamide: A classical hallucinogenic drug first synthesized in 1938 from ergotamine, an alkaloid of the ergot rye fungus (Albert Hofmann 1969).

MEQ30 30-item revised mystical experience questionnaire

MTE ‘mystical-type’ experience: Subjective experiences whose characteristics include a sense of connectedness, transcendence, and ineffability.

PCI Phenomenology of Consciousness Inventory: A psychometric questionnaire based on the hypothesis that different states of consciousness can be characterized in terms of phenomenological dimensions which can be quantified in terms of their intensity. The resulting pattern is assumed to be typical of a particular induction method and can be observed consistently (Figueiredo et al. 2016).

RAM random-access memory

RDG rendering dependency graph: **UE4**’s graph-based scheduling system to perform whole-frame optimization of the render pipeline.

THC tetrahydrocannabinol: One of the psychoactive compounds in cannabis.

UE4 Unreal Engine 4: A game development engine.

VAS visual analog scale

VR virtual reality

fBm fractional Brownian motion

Bibliography

- Aday, Jacob S, Christopher C Davoli, and Emily K Bloesch. 2020. "Psychedelics and virtual reality: parallels and applications." *Therapeutic Advances in Psychopharmacology* 10:2045125320948356.
- Albert Hofmann. 1969. "LSD: Completely Personal." Accessed December 6, 2013. <https://web.archive.org/web/20131206032629/http://www.maps.org/news-letters/v06n3/06346hof.html>.
- Alessa Baker. 2021. "CustomShaderDirectoryExample: An example project for a tutorial on adding a custom shader directory." Accessed May 18, 2022. <https://github.com/Sythenz/CustomShaderDirectoryExample>.
- Anderson, WH, and John E O'Malley. 1972. "Trifluoperazine for the trailing phenomenon." *JAMA* 220 (9): 1244–1245.
- Bartossek, Marie Therese, Johanna Kemmerer, and Timo Torsten Schmidt. 2021. "Altered states phenomena induced by visual flicker light stimulation." *Plos one* 16 (7): e0253779.
- Bengio, Yoshua. 2017. "The consciousness prior." *arXiv preprint arXiv:1709.08568*.
- Bensemman, Joshua, and Michael Witbrock. 2021. "The effects of implementing phenomenology in a deep neural network." *Heliyon* 7 (6): e07246.
- Block, Ned. 1993. "Consciousness Explained by Daniel C. Dennett." *The Journal of Philosophy* 90 (4): 181–193.
- Carbonaro, Theresa M, Matthew W Johnson, Ethan Hurwitz, and Roland R Griffiths. 2018. "Double-blind comparison of the two hallucinogens psilocybin and dextromethorphan: similarities and differences in subjective experiences." *Psychopharmacology* 235 (2): 521–534.
- Crick, Francis, and Christof Koch. 1990. "Towards a neurobiological theory of consciousness." In *Seminars in the Neurosciences*, 2:263–275. Saunders Scientific Publications.
- Dehaene, Stanislas. 2014. *Consciousness and the brain: Deciphering how the brain codes our thoughts*. Penguin.
- Dittrich, Adolf. 1998. "The standardized psychometric assessment of altered states of consciousness (ASCs) in humans." *Pharmacopsychiatry* 31 (S 2): 80–84.
- Dittrich, Adolf, Daniel Lamparter, and Maja Maurer. 2010. "5D-ASC: Questionnaire for the assessment of altered states of consciousness." *A short introduction. Zurich, Switzerland: PSIN PLUS*.

- Díaz, José Luis. 2010. "Sacred plants and visionary consciousness." *Phenomenology and the Cognitive Sciences* 9 (2): 159–170.
- Drempetic, Cassandra, and Leigh Ellen Potter. 2017. "Wearable bass tactile sound systems and immersion." In *Proceedings of the 29th Australian Conference on Computer-Human Interaction*, 576–580.
- Enhance Experience Inc. 2016. "Rez Infinite." Accessed March 6, 2022. <https://web.archive.org/web/20220306195027/https://rezinfinite.com/>.
- Figueiredo, Renato Garita, Hendrik Berkemeyer, Katharina Dworatzky, and Timo T Schmidt. 2016. "Building a unifying database to enable flexible meta-analyses of data on altered states of consciousness."
- Filip Tylš, Tomáš Páleníček Zuzana Postránecká Vladěna Sobasová Tereza Klučková Michal Šenk Jan Jarčík Filip Aura, Vojtěch Viktorin. 2020. "Promotional page for the iTrip smartphone application." Accessed May 4, 2022. <https://web.archive.org/web/20220504085651/https://itrip.psyres.eu/>.
- Fischer, Rico, RM Hill, and Diana Warshay. 1969. "Effects of the psychodysleptic drug psilocybin on visual perception. Changes in brightness preference." *Experientia* 25 (2): 166–169.
- Fischer, Roland, Richard Hill, Karen Thatcher, and James Scheib. 1970. "Psilocybin-induced contraction of nearby visual space." *Agents and actions* 1 (4): 190–197.
- Furukawa, Taichi, Nobuhisa Hanamitsu, Yoichi Kamiyama, Hideaki Nii, Charalampos Krekoulotis, Kouta Minamizawa, Akihito Noda, Junko Yamada, Keiichi Kitamura, Daisuke Niwa, et al. 2019. "Synesthesia Wear: Full-body haptic clothing interface based on two-dimensional signal transmission." In *SIGGRAPH Asia 2019 Emerging Technologies*, 48–50.
- Glowacki, David R, Mark D Wonnacott, Rachel Freire, Becca R Glowacki, Ella M Gale, James E Pike, Tiu de Haan, Mike Chatziapostolou, and Oussama Metatla. 2020. "Is-ness: using multi-person VR to design peak mystical type experiences comparable to psychedelics." In *Proceedings of the 2020 CHI Conference on Human Factors in Computing Systems*, 1–14.
- Greco, Antonino, Giuseppe Gallitto, Marco D'Alessandro, and Clara Rastelli. 2021. "Increased Entropic Brain Dynamics during DeepDream-Induced Altered Perceptual Phenomenology." *Entropy* 23 (7): 839.
- Guerra-Doce, Elisa. 2015. "Psychoactive substances in prehistoric times: examining the archaeological evidence." *Time and Mind* 8 (1): 91–112.
- Hartman, Alan M, and Leo E Hollister. 1963. "Effect of mescaline, lysergic acid diethylamide and psilocybin on color perception." *Psychopharmacologia* 4 (6): 441–451.
- Hill, Richard M, and Roland Fischer. 1973. "Induction and extinction of psilocybin induced transformations of visual space." *Pharmacopsychiatry* 6 (04): 258–263.
- Hill, RM, Roland Fischer, and Diana Warshay. 1969. "Effects of excitatory and tranquilizing drugs on visual perception. Spatial distortion thresholds." *Experientia* 25 (2): 171–172.

- Holze, Friederike, Patrick Vizeli, Laura Ley, Felix Müller, Patrick Dolder, Melanie Stocker, Urs Duthaler, Nimmy Varghese, Anne Eckert, Stefan Borgwardt, et al. 2021. "Acute dose-dependent effects of lysergic acid diethylamide in a double-blind placebo-controlled study in healthy subjects." *Neuropsychopharmacology* 46 (3): 537–544.
- Holze, Friederike, Patrick Vizeli, Felix Müller, Laura Ley, Raoul Duerig, Nimmy Varghese, Anne Eckert, Stefan Borgwardt, and Matthias E Liechti. 2020. "Distinct acute effects of LSD, MDMA, and D-amphetamine in healthy subjects." *Neuropsychopharmacology* 45 (3): 462–471.
- Hutten, Nadia RPW, Natasha L Mason, Patrick C Dolder, Eef L Theunissen, Friederike Holze, Matthias E Liechti, Amanda Feilding, Johannes G Ramaekers, and Kim PC Kuypers. 2020. "Mood and cognition after administration of low LSD doses in healthy volunteers: a placebo controlled dose-effect finding study." *European Neuropsychopharmacology* 41:81–91.
- Jain, Anil K. 1989. *Fundamentals of digital image processing*. Prentice-Hall, Inc.
- Johnson, Justin, Alexandre Alahi, and Li Fei-Fei. 2016. "Perceptual losses for real-time style transfer and super-resolution." In *European conference on computer vision*, 694–711. Springer.
- Karras, Tero, Samuli Laine, and Timo Aila. 2019. "A Style-Based Generator Architecture for Generative Adversarial Networks." In *Proceedings of the IEEE/CVF Conference on Computer Vision and Pattern Recognition (CVPR)*. June.
- Kitson, Alexandra, Steve DiPaola, and Bernhard E Riecke. 2019. "Lucid Loop: a virtual deep learning biofeedback system for lucid dreaming practice." In *Extended Abstracts of the 2019 CHI Conference on Human Factors in Computing Systems*, 1–6.
- Kleinman, Joel Edward, John Christian Gillin, and Richard Jed Wyatt. 1977. "A comparison of the phenomenology of hallucinogens and schizophrenia from some autobiographical accounts." *Schizophrenia Bulletin* 3 (4): 560.
- Klüver, H. 1966. *Mescal and mechanisms of hallucinations* Chicago.
- Klüver, Heinrich. 1942. "Mechanisms of hallucinations."
- Kometer, Michael, and Franz X Vollenweider. 2016. "Serotonergic hallucinogen-induced visual perceptual alterations." *Behavioral neurobiology of psychedelic drugs*: 257–282.
- Konishi, Yukari, Nobuhisa Hanamitsu, Benjamin Outram, Youichi Kamiyama, Kouta Minamizawa, Ayahiko Sato, and Tetsuya Mizuguchi. 2016. "Synesthesia suit." In *International AsiaHaptics conference*, 499–503. Springer.
- Konishi, Yukari, Nobuhisa Hanamitsu, Benjamin Outram, Kouta Minamizawa, Tetsuya Mizuguchi, and Ayahiko Sato. 2016. "Synesthesia suit: the full body immersive experience." In *ACM SIGGRAPH 2016 VR Village*, 1–1.
- Lang, Tom. 2004. *Twenty statistical errors even you can find in biomedical research articles*.
- Leuner, Hanscarl. 1962. "Die experimentelle Psychose."
- Ludwig, Arnold M. 1966. "Altered states of consciousness." *Archives of general Psychiatry* 15 (3): 225–234.

- Madary, Michael, and Thomas K Metzinger. 2016. "Real virtuality: a code of ethical conduct. Recommendations for good scientific practice and the consumers of VR-technology." *Frontiers in Robotics and AI* 3:3.
- Manske, Richard HF. 1931. "A synthesis of the methyltryptamines and some derivatives." *Canadian Journal of Research* 5 (5): 592–600.
- Mark Hay. 2020. "The Colonization of the Ayahuasca Experience." Accessed February 7, 2022. <https://web.archive.org/web/20220207102112/https://daily.jstor.org/the-colonization-of-the-ayahuasca-experience/>.
- Masters, Robert, and Jean Houston. 2000. *The varieties of psychedelic experience: The classic guide to the effects of LSD on the human psyche*. Simon / Schuster.
- Metzinger, Thomas. 2009. *The ego tunnel: The science of the mind and the myth of the self*. Basic Books (AZ).
- Mordvintsev, Alexander, Christopher Olah, and Mike Tyka. 2015. "Inceptionism: Going deeper into neural networks."
- Northoff, Georg. 2011. "Self and brain: what is self-related processing?" *Trends in cognitive sciences* 15 (5): 186–187.
- Olano, Mark, John C Hart, Wolfgang Heidrich, Bill Mark, and Ken Perlin. 2002. "Real-time shading languages." SIGGRAPH.
- Ossi Luoto. 2021. "SceneViewExtTest: Unreal Engine 4.26 test project and plugin for SceneViewExtension and how to hook custom shaders to RDG/GraphBuilder." Accessed May 19, 2022. <https://github.com/A57R4L/SceneViewExtTest>.
- Outram, Benjamin, Yukari Konishi, Aria Shimbo, Reiko Shimizu, Kouta Minamizawa, Ayahiko Sato, and Tetsuya Mizuguchi. 2017. "Crystal Vibes feat. Ott: A psychedelic musical virtual reality experience utilising the full-body vibrotactile haptic synesthesia suit." In *2017 23rd International Conference on Virtual System & Multimedia (VSMM)*, 1–4. IEEE.
- Perlin, Ken. 1985. "An image synthesizer." *ACM Siggraph Computer Graphics* 19 (3): 287–296.
- Preller, Katrin H, and Franz X Vollenweider. 2016. "Phenomenology, structure, and dynamic of psychedelic states." *Behavioral neurobiology of psychedelic drugs*: 221–256.
- PsychonautWiki. 2020. *Acuity enhancement — PsychonautWiki, The Open Encyclopedia of Psychonautics*. Accessed May 19, 2022. https://web.archive.org/web/20220519164532/https://psychonautwiki.org/wiki/Acuity_enhancement.
- PsychonautWiki. 2021. "Replication index — PsychonautWiki, The Open Encyclopedia of Psychonautics." Accessed April 30, 2022. https://web.archive.org/web/20220430191911/https://psychonautwiki.org/wiki/Replication_index.
- Rastelli, Clara, Antonino Greco, Yoed N Kenett, Chiara Finocchiaro, and Nicola De Pisapia. 2021. "Simulated visual hallucinations in virtual reality enhance cognitive flexibility." *bioRxiv*.
- Reggia, James A, Garrett E Katz, and Gregory P Davis. 2020. "Artificial conscious intelligence." *Journal of Artificial Intelligence and Consciousness* 7 (01): 95–107.

- Schartner, Michael M, and Christopher Timmermann. 2020. "Neural network models for DMT-induced visual hallucinations." *Neuroscience of Consciousness* 2020 (1): niaa024.
- Schmidt, TT, and Tomislav Majić. 2018. "Empirische Untersuchung veränderter Bewusstseinszustände." In *Handbuch Psychoaktive Substanzen*, 153–171. Springer.
- Siegel, Ronald K, and Murray E Jarvik. 1975. "Drug-induced hallucinations in animals and man." *Hallucinations: Behavior, experience and theory* 81:161.
- Studerus, Erich, Alex Gamma, and Franz X Vollenweider. 2010. "Psychometric evaluation of the altered states of consciousness rating scale (OAV)." *PloS one* 5 (8): e12412.
- SUBPAC. 2013. "The SUBPAC front page." Accessed February 27, 2022. <https://web.archive.org/web/20220227213936/https://subpac.com/>.
- Suzuki, Keisuke, Warrick Roseboom, David J Schwartzman, and Anil K Seth. 2018. "Hallucination Machine: Simulating Altered Perceptual Phenomenology with a Deep-Dream Virtual Reality platform." In *ALIFE 2018: The 2018 Conference on Artificial Life*, 111–112. MIT Press.
- Synesthesia Lab. 2016. "The Synesthesia Suit product page." Accessed February 27, 2022. <https://web.archive.org/web/20220227212257/https://synesthesia-suit.com/>.
- Synesthesia Lab. 2021. "The Synesthesia X1 - 2.44 product page." Accessed February 27, 2022. <https://web.archive.org/web/20220227211421/https://synesthesialab.com/x/>.
- Weinel, Jonathan. 2011. "Quake delirium: remixing psychedelic video games." *Sonic Ideas/Ideas Sonicas* 3 (2).
- Weinel, Jonathan, Stuart Cunningham, Nathan Roberts, Darryl Griffiths, and Shaun Roberts. 2015. "Quake delirium EEG." In *2015 Internet Technologies and Applications (ITA)*, 335–338. IEEE.
- Zimmermann, Marc, Volker Helzle, and Diana Arellano. 2016. "Longing for wilderness." In *ACM SIGGRAPH 2016 VR Village*, 1–2.

A | Questionnaire

Czech translation

The translated questionnaire consisted of the following 94 questions, with responses in the form of horizontal visual analogue scales, with the left side of the scale labeled as “Ne, ne více než obvykle” (“No, not more than usually”) and the right side as “Ano, více než obvykle” (“Yes, much more than usually”).

Question

1. Cítil/a jsem, že jsem byl/a v nádherném jiném světě.
2. Moje myšlení a jednání bylo zpomalené.
3. Moje tělesné pocity byly velice příjemné.
4. Slyšel/a jsem jednotlivá slova, aniž bych věděl/a odkud přicházejí.
5. Slyšel/a jsem zvonění a tóny, aniž bych věděl/a odkud přicházejí.
6. Cítil/a jsem, jako by mne ovládly temné síly.
7. Viděl/a jsem věci, o kterých jsem věděl/a, že nejsou skutečné.
8. Cítil/a jsem se jako loutka nebo panenka.
9. Cítil/a jsem se být propojen/á s vyšší mocí.
10. Cítil/a jsem se ospalý/á.
11. V mysli mi vytanula melodie, kterou jsem si musel/a neustále opakovat dokola.
12. Zažil/a jsem pocit bezbřehé radosti.
13. Bezvýznamné zvuky zněly jako opravdová slova nebo věty.
14. V absolutní tmě nebo se zavřenýma očima jsem viděl/a pravidelné obrazce.
15. Cítil/a jsem se opilý/á.
16. Cítil/a jsem, že jsem byl/a jako zázrakem navždy změněn/a.
17. Cítil/a jsem se na pokraji bezvědomí.
18. Zdálo se mi, že se vše sjednocuje v jedno.
19. Slyšel/a jsem svoje myšlenky, jako kdybych je říkal/a nahlas.
20. Zdálo se, že zvuky ovlivňují to, co vidím.
21. Cítil/a jsem se ztrápený/á.
22. Se zavřenýma očima nebo v absolutní tmě jsem viděl/a barvy.
23. Zdálo se, že tvary se mění podle zvuků.
24. Vnímál/a jsem vše rozmazaně, jakoby skrze nějakou mlhu.
25. Někáký hlas komentoval vše, na co jsem pomyslel/a, přestože kolem nikdo nebyl.
26. Měl/a jsem pocit, jako bych už neměl/a tělo.
27. Cítil/a jsem se neschopný/á udělat sebemenší rozhodnutí.
28. Některé každodenní záležitosti získaly zvláštní význam.
29. Cítil/a jsem se mátožný.
30. Slyšel/a jsem celé věty, aniž bych věděla, odkud přicházejí.
31. Věci kolem pro mě dostaly nový zvláštní význam.
32. Bá/a jsem se, že stav, ve kterém jsem se nacházel/a, bude trvat navždy.
33. V absolutní tmě nebo se zavřenýma očima jsem viděl/a světla nebo záblesky.
34. Cítil/a jsem se sjednocen/a se svým okolím.
35. Starosti a úzkosti každodenního života se zdály nepodstatné.
36. Moje vnímání času a prostoru bylo změněné, jako kdybych snil/a.
37. Moje vnímání bylo rozmazané.
38. Měl/a jsem problém odlišit podstatné věci od nepodstatných.
39. Se zavřenýma očima nebo v absolutní tmě se mi promítaly různé scény.
40. Cítil/a jsem, že mám mimořádné schopnosti.
41. Zažil/a jsem dotek věčnosti.

42. Zdálo se, že konflikty a rozpory se rozplynuly.
43. Byl/a jsem vyděšený/á, aniž bych přesně věděl/a proč.
44. Všechno jsem prožíval/a děsivě zkreslené.
45. Svět se zdál mimo dobro a zlo.
46. Své okolí jsem zažíval/a jako divné a zvláštní.
47. Cítil/a jsem se jako bych byl/a paralizovaný/á.
48. Slyšel/a jsem hudbu, aniž bych věděl/a, odkud přichází.
49. Slyšel/a jsem něco tak slabě, že jsem to nemohl/a identifikovat.
50. Cítil/a jsem vše velmi intenzivně.
51. Cítil/a jsem se otupělý/á.
52. Prožíval jsem minulost, současnost a budoucnost jako jedno.
53. Zažil/a jsem nesnesitelnou prázdnotu.
54. Okolní předměty mě emočně upoutávaly více než obvykle.
55. Z původně nejasného šumu, jež jsem měl/a problém identifikovat, se postupně vyvinuly jasné tóny a zvonění.
56. Cítil/a jsem se ohrožen/a.
57. Spousta věcí mi připadala neskonale krásná.
58. Na mysl mi přišly věci, o kterých jsem si myslel/a, že jsou již dlouho zapomenuté.
59. Cítil/a jsem se, jako se obvykle cítím těsně před usnutím.
60. Moje tělo se cítilo strnulé, bez života a/nebo jako cizí.
61. Cítil/a jsem se jako v polospánku.
62. Měl/a jsem pocit, že jsem mimo své tělo.
63. Připadalo mi, jako bych se vznášel/a.
64. Cítil/a jsem se izolovaný/á od všeho a od všech.
65. Slyšel/a jsem hlasy, které nepřicházely z okolí jako obvykle.
66. Slyšel/a jsem něco jako hučení, bzučení nebo šumění, aniž bych dokázal/a rozpoznat jejich příčinu.
67. Nebyl/a jsem schopen/á dokončit myšlenku, moje myšlení bylo opakovaně nesouvislé.
68. Cítil/a jsem, že každou chvíli usnu.
69. Najednou jsem pochopil/a souvislosti, které mě předtím mátlly.
70. Mnoho věcí mi připadalo neuvěřitelně legračních.
71. Zdálo se, že hranice mezi mnou a mým okolím se stírá.
72. Mohl/a jsem neobyčejně jasně vidět obrazy ze svých vzpomínek a představ.
73. Cítil/a jsem se naprosto volný/á a zproštěný/á veškerých povinností.
74. Slyšel/a jsem neurčité zvuky, aniž bych věděl/a, odkud přicházejí.
75. Zdálo se, že barvy věcí se mění podle zvuků a hluku.
76. Zvuky a hluk byly slabší než obvykle.
77. Měl/a jsem velice originální myšlenky.
78. Měl/a jsem pocit, že už vůbec nemám vlastní vůli.
79. Báł/a jsem se, že nad sebou ztrácím kontrolu.
80. Po delší časový úsek jsem zůstal/a ustrnulý/á ve velice nepřírozené pozici.
81. Zažil/a jsem něco jako silný úžas.
82. Moje představivost byla extrémně živá.
83. Věci v mém okolí se mi zdály menší nebo větší.
84. Cítil/a jsem se vyčerpaný/á.
85. Čas ubíhal trýznivě pomalu.
86. Prožil/a jsem hluboký vnitřní klid.
87. Všechno kolem mě se zdálo být živoucí.
88. Všechno utíkalo tak rychle, že jsem to nestačil/a sledovat.
89. Měl/a jsem pocit, že se stane něco hrozného.
90. Byl/a jsem schopný/á si vybavit určité události s extrémní jasností.
91. Zažil/a jsem všeobíhající lásku.
92. V místnosti jsem zaznamenal/a zvuky, u kterých nepovažuji za pravděpodobné, že by byly skutečné.
93. Slyšel/a jsem tikání, klepání, zvonění nebo rachocení, aniž bych byl/a schopný/á rozpoznat jejich příčinu.
94. Můj prožitek měl i náboženský rozměr.

Question per Factor Influence

The following factors of the questionnaire scorings are influenced by the questions indicated by the indices on the right of each factor.

5-Dimensional Altered States of Consciousness Questionnaire (5D-ASC)

Factor	Question Indices
1. Experience of Unity	18, 34, 41, 42, 52
2. Spiritual Experience	9, 81, 94
3. Blissful State	12, 86, 91
4. Insightfulness	50, 69, 77
5. Disembodiment	26, 62, 63
6. Impaired Control and Cognition	8, 27, 38, 47, 64, 67, 78
7. Anxiety	32, 43, 44, 46, 56, 89
8. Complex Imagery	39, 79, 82
9. Elementary Imagery	14, 22, 33
10. Audio-Visual Synesthesia	20, 23, 75
11. Changed Meaning of Percepts	28, 31, 54

11-Factor Altered States of Consciousness Questionnaire (11-ASC)

Factor	Question Indices
1. Oceanic Boundlessness	1, 3, 9, 12, 16, 18, 26, 34, 35, 36, 40, 41, 42, 45, 50, 52, 57, 62, 63, 69, 71, 73, 81, 86, 87, 91, 94
2. Dread of Ego Dissolution	6, 8, 21, 27, 32, 38, 43, 44, 46, 47, 53, 56, 60, 64, 67, 78, 79, 80, 85, 88, 89
3. Visionary Restructuazilation	7, 14, 20, 22, 23, 28, 31, 33, 39, 54, 58, 70, 72, 75, 77, 82, 83, 90
4. Auditory Alterations	4, 5, 11, 13, 19, 25, 30, 48, 49, 55, 65, 66, 74, 76, 92, 93
5. Vigilance Reduction	2, 10, 15, 17, 24, 29, 37, 51, 59, 61, 68, 84

B | Informed Consent Form

The following page contains the informed consent form in czech. Notably, as the rest of the study, it takes into account the *Recommendations for good scientific practice and the consumers of VR-technology* (Madary and Metzinger 2016).

Informovaný souhlas

Informace o studii (projektu):

Název studie: SimR, Simulace pozměněných stavů vědomí pomocí virtuální reality

Autor studie: Jakub Hlusička, student ČVUT

Cíle studie:

Cílem této studie je změřit vliv vyvinuté aplikace pro imerzivní virtuální realitu (dále jen VR aplikace) na lidské vědomí. VR aplikace byla vytvořena za účelem simulace či napodobení vybraných aspektů pozměněných stavů vědomí, a to konkrétně takových, které vznikají po užití psychedelických látek, jako je např. psilocybin (aktivní látka v lysohlávkách) nebo LSD.

Průběh testování:

Testování proběhne dvakrát, v různých dnech. Jednou se testuje aktivní scénář, kdy se uživateli spustí simulace pozměněného stavu vědomí; jednou kontrolní scénář, kdy se pozměněný stav vědomí nesimuluje.

Před testovací fází jsou během 5-10 minut předány instrukce k použití technologií virtuální reality a použití vyvinuté VR aplikace. Testovací fáze trvá 10 minut. Po testovací fázi je účastníkovi předán dotazník k vyplnění.

Informace o účastníkovi:

Jméno: _____

Datum narození: _____

Prohlášení:

1. Já, níže podepsaný(á) souhlasím s mou účastí ve studii. Je mi více než 18 let.
2. Rozumím, že technologie imerzivní virtuální reality mohou trvale ovlivnit chování uživatele a že některá tato rizika technologií imerzivní virtuální reality mohou být v současné době neznámá.
3. Rozumím, že VR aplikace nemusí plně odpovídat pozměněným stavům vědomí vyvolaných pomocí psychedelických látek a že mě moje účast v této studii a studie samotná nepodněcuje k užití psychedelických látek.
4. Při zařazení do studie budou moje osobní data uchována s plnou ochranou důvěrnosti dle platných zákonů ČR. Je zaručena ochrana důvěrnosti mých osobních dat. Při vlastním provádění studie mohou být osobní údaje poskytnuty jiným než výše uvedeným subjektům pouze bez identifikačních údajů. Rovněž pro výzkumné a vědecké účely mohou být moje osobní údaje poskytnuty pouze bez identifikačních údajů (anonymní data) nebo s mým výslovným souhlasem.
5. Porozuměl(a) jsem tomu, že mé jméno se nebude nikdy vyskytovat v referátech o této studii. Já naopak nebudu proti použití výsledků z této studie.
6. Byl(a) jsem podrobně informován(a) o cíli studie, o jejích postupech, okolnostech, průběhu a délce trvání.
7. Porozuměl(a) jsem tomu, že svou účast ve studii mohu kdykoliv přerušit či odstoupit. Moje účast ve studii je dobrovolná.

Datum:

Podpis účastníka:

C | Remarks on the Method of Statistical Analysis

Many studies utilizing the 5D-ASC scoring or the 11-ASC scoring (such as Carbonaro et al. (2018), Holze et al. (2020), Holze et al. (2021), and Hutten et al. (2020)) use statistical tests which require normally distributed variables (repeated-measures analysis of variance, paired t-test), to compare the resulting questionnaire scores of placebo and non-placebo groups. Our study has used the same approach, but we identified an issue with this approach, which may be relevant to the field.

The issue stems from the fact that the visual analog scale (VAS), which is the method participants answer to the questions of the questionnaire, results in bounded measurements in the interval $[0\%; 100\%]$. After applying this questionnaire in our study, we found out, that for the control scenario, many of the questions were answered with 0%, as can also be seen in the aforementioned studies. This results in the mean of the resulting factors, which are also bounded by the same interval as the answers themselves, being very close to the lower bound of 0%.

It may be a mistake to assume that the resulting factors are normally distributed, if, for example, their 95% confidence interval (of the assumed normal distribution) reaches outside of the $[0\%; 100\%]$ bounds. This can also be seen in figures 4.1 and 4.2. It seems that some studies prefer to mask this issue by visualising the error of the resulting factors using the standard error (SE), which is essentially a 68% confidence interval. However, the preferred measure for precision in medicine is the 95% confidence interval (Lang 2004), so the usage of the SE may be misleading. When interpreting data with the SE, it helps to remember that the 95% confidence interval of a normal distribution is roughly twice (~ 1.96) as large as the 68% interval denoted by the SE.

As an alternative, it may be much more appropriate to use a bounded distribution to model the resulting factors instead. The following two may be suitable:

1. The logit-normal distribution: If X is logit-normally distributed, then $Y = \text{logit}(X) = \ln\left(\frac{X}{1-X}\right)$ is normally distributed. Essentially, the logit transform stretches the lower (0) and upper (1) bounds to infinity (see figure C.1). However, the logit transform's domain is an open interval $(0; 1)$, rather than a closed interval $[0; 1]$, which prevents it from being usable with measurements at the bounds. This is, unfortunately, the case for the psychometric questionnaire used in this study, as participants may answer with 0% or 100%.
2. The beta distribution: Doesn't suffer from the necessity of using a transform that would be undefined at the bounds. Possibly even more expressive than the logit-

normal distribution.

I suspect the main challenge of using these alternative distributions comes with the testing of hypotheses. With these distributions, we can no longer use standard statistical methods of analysis only applicable to normally distributed data.

I don't believe this finding invalidates past studies, but it may serve as a place for improvement of future ones.

Figure C.1: The logit transform.

(a) (b)
 Ex- The
 am-cor-
 plesre-
 of spond-
 logitag
 normal-
 dis-mal
 tri- dis-
 bu- tri-
 tionbu-
 of tions
 ran-of
 don't =
 $\text{varilogit}(X)$.
 able
 X .

Figure C.2: Examples of the logit-normal distribution and their corresponding normal distributions.

Figure C.3: Examples of the beta distribution. Note that the beta distribution, as opposed to the logit-normal distribution, is also able to express a uniform distribution with parameters $\alpha = 1, \beta = 1$.